FINE STRUCTURE

OF β-DECAY STRENGTH FUNCTION $S_{\beta}(E)$

The probability of the β transition is proportional to the product of the lepton part described by the Fermi function $f(Q_\beta - E)$ and the nucleon part described by the β transition strength function $S_\beta(E)$. The function $S_\beta(E)$ is one of the most important characteristics of the atomic nucleus defined as the distribution of the moduli squared of the matrix elements of the β-decay type in nuclear excitation energy E.

Information on the structure of $S_\beta(E)$ is important for many nuclear physics areas. Reliable experimental data on the structure of $S_\beta(E)$ are necessary for predicting half-lives of nuclei far from the stability line, verifying completeness of decay schemes, calculating energy release from decay of fission products in nuclear reactors, calculating spectra of delayed particles, calculating the delayed fission probability and evaluating fission barriers for nuclei far from the β stability line, calculating production of various elements in astrophysical processes, and developing microscopic models for calculation of $S_\beta(E)$, especially in deformed nuclei.

Until recently, experimental investigations of the $S_\beta(E)$ structure were carried out using total absorption gamma-ray spectrometers (TAGS) and total absorption spectroscopy methods, which had low energy resolution. With TAGS spectroscopy, it became possible to demonstrate experimentally the resonance structure of $S_\beta(E)$ for Gamow–Teller β transitions.

Yu.V. Naumov, A.A. Bykov, I.N. Izosimov, *Sov.J.Part.Nucl.*, 14,175(1983).

However, TAGS methods have some disadvantages arising from low energy resolution of NaI-based spectrometers. Modern experimental instruments allow using nuclear spectroscopy methods with high energy resolution to study the fine structure of $S_\beta(E)$.

I.N. Izosimov, V.G. Kalinnikov, A.A. Solnyshkin, *Phys. Part. Nucl.*, 42, 1804(2011). DOI:10.1134/S1063779611060049

High-resolution nuclear spectroscopy methods, like total absorption gamma spectroscopy (TAGS) methods, give conclusive evidence of the resonance structure of $S_\beta(E)$ for GT transitions in both spherical and deformed nuclei. High-resolution nuclear spectroscopy methods made it possible to demonstrate experimentally the resonance nature of $S_\beta(E)$ for FF transitions and reveal splitting of the peak in the strength function for the GT β^+/EC decay of the deformed nucleus into two components. This splitting indicates anisotropy of oscillation of the isovector density component.

For the GT-β transitions, FF-β transitions in the ξ approximation (Coulomb approximation), and unique FF-β transitions the $T_{1/2}$, ft, level populations I(E), $S_\beta(E)$ and reduced probabilities B(GT), $[B(\lambda\pi = 0^-)+B(\lambda\pi=1^-)]$, $[B(\lambda\pi = 2^-)]$ are related as follows :

$$d(I(E))/dE = S_\beta(E)\, T_{1/2}\, f(Q_\beta - E), \qquad (1)$$

$$(T_{1/2})^{-1} = \int S_\beta(E) f(Q_\beta - E)\, dE, \qquad (2)$$

$$\int_{\Delta E} S_\beta(E) dE = \sum_{\Delta E} 1/(ft). \qquad (3)$$

$$B(GT,E)=(g^{eff}{}_A)^2/4\pi \left| \langle I_f \| \sum t_\pm(k)\, \sigma_\mu(k) \| I_i \rangle \right|^2 /(2I_i+1), \qquad (4)$$

$$B(GT,E)=[D(g^2{}_V/4\pi)]/ft, \qquad (5)$$

$$[B(\lambda\pi =0^-) + B(\lambda\pi =1^-)] = [D\, g^2{}_V/4\pi]/ft, \qquad (6)$$

$$[B(\lambda\pi=2^-)]=3/4[Dg^2{}_V/4\pi]/ft, \qquad (7)$$

where $S_\beta(E)$ – the beta decay strength function which describe the nuclear part of transition, $f(Q - E)$ – the Fermi function which describe the lepton part of transition and Q – is the total energy of the beta decay.

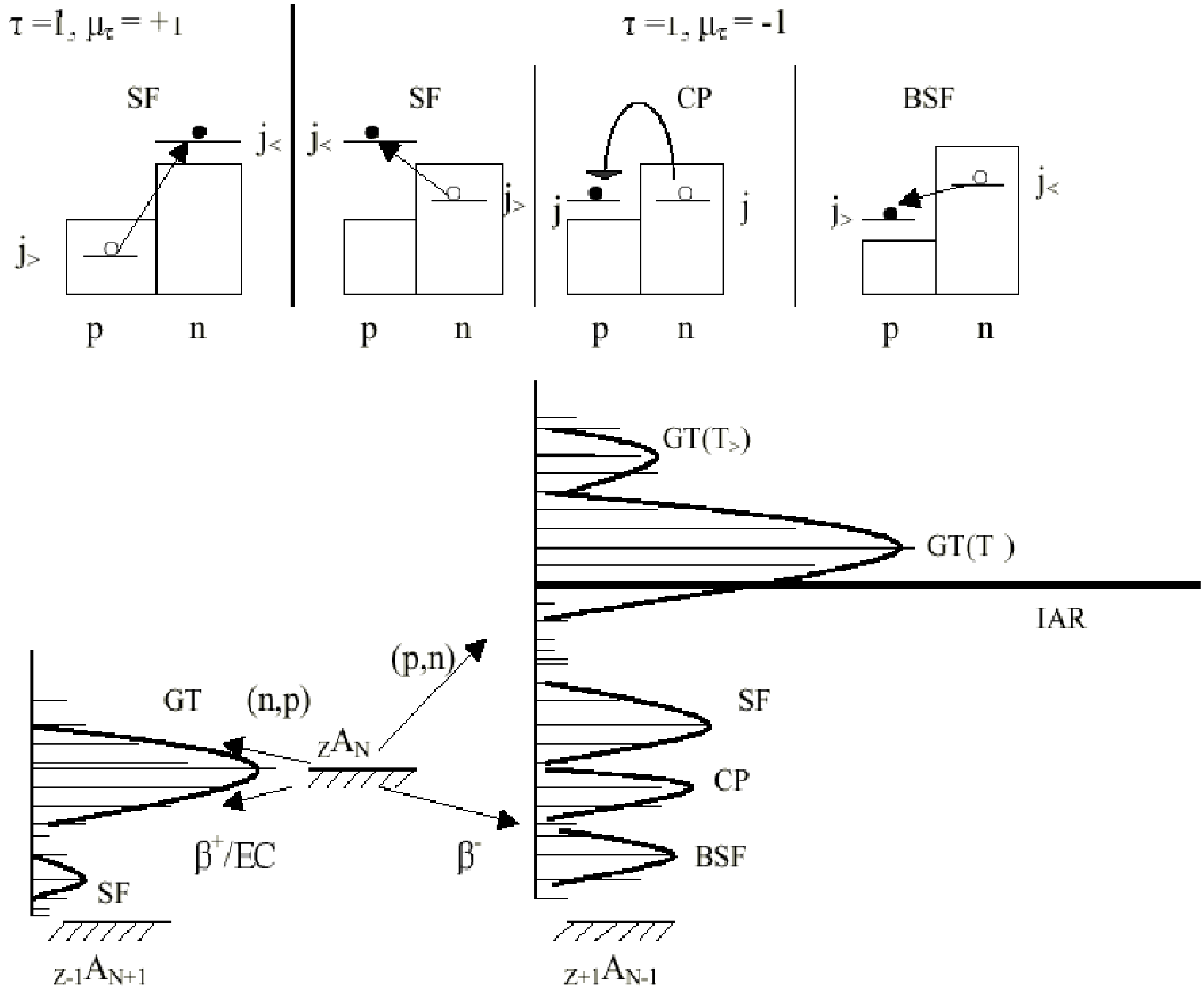

τ =1, μτ = +1
τ =1, μτ = -1
SF
SF
CP
BSF
j<
j>
j<
j>
j
j
j<
j>
p n
p n
p n
p n
GT(T>)
GT(T)
IAR
(p,n)
GT (n,p)
zAN
SF
CP
BSF
β+/EC
β-
SF
Z-1AN+1
Z+1AN-1

Nuclear spectroscopy methods with high energy resolution to study the fine structure of $S_\beta(E)$

•**GT** and **FF** $S_\beta(E)$ has resonances both for spherical, transition, and deformed nuclei.

•Deformation leads to the splitting of the $S_\beta(E)$ peaks.

•Anisotropy of the spin–isospin density oscillations results in the difference of oscillation energies $< E >_\gamma - < E >_\beta$ of proton holes against neutron particles perpendicular to the symmetry axis and along symmetry axis. In the deformed ^{160}Dy nucleus $< E >_\gamma - < E >_\beta$ is about 1 MeV.

I.N. Izosimov, V.G. Kalinnikov, F.F. Solnyshkin *Phys. Part. Nucl.*, 42, 1804(2011).
DOI:10.1134/S1063779611060049

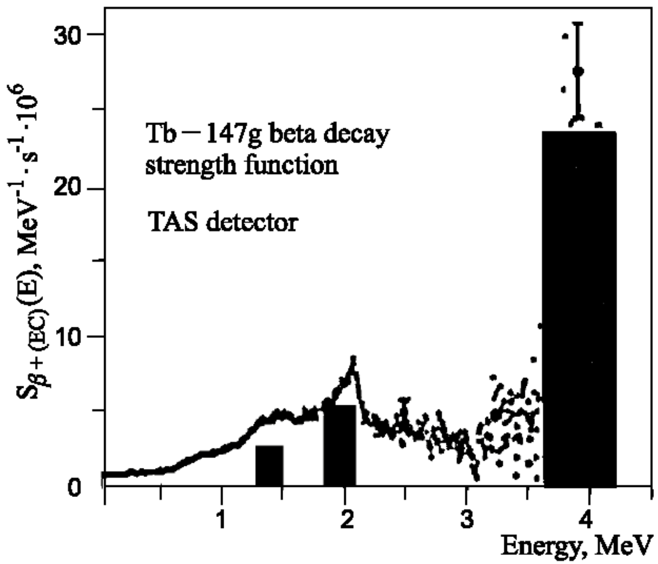
Tb − 147g beta decay
strength function
TAS detector
$S_{\beta+(EC)}(E)$, $MeV^{-1}\cdot s^{-1}\cdot 10^{6}$
Energy, MeV
0
10
20
30
1
2
3
4

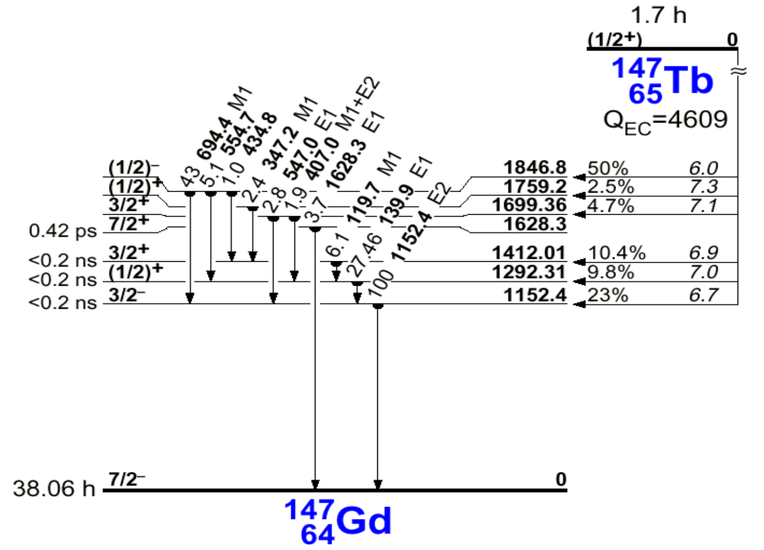
1.7 h
(1/2+) 0
$^{147}_{65}$Tb
Q_{EC}=4609
694.4 M1
554.7
434.8
347.2 M1
547.0 E1
407.0 M1+E2
1628.3 E1
119.7 M1
139.9 E1
1152.4 E2
(1/2)− 1846.8 50% 6.0
(1/2)+ 1759.2 2.5% 7.3
3/2+ 1699.36 4.7% 7.1
0.42 ps 7/2+ 1628.3
<0.2 ns 3/2+ 1412.01 10.4% 6.9
<0.2 ns (1/2)+ 1292.31 9.8% 7.0
<0.2 ns 3/2− 1152.4 23% 6.7
38.06 h 7/2− 0
$^{147}_{64}$Gd

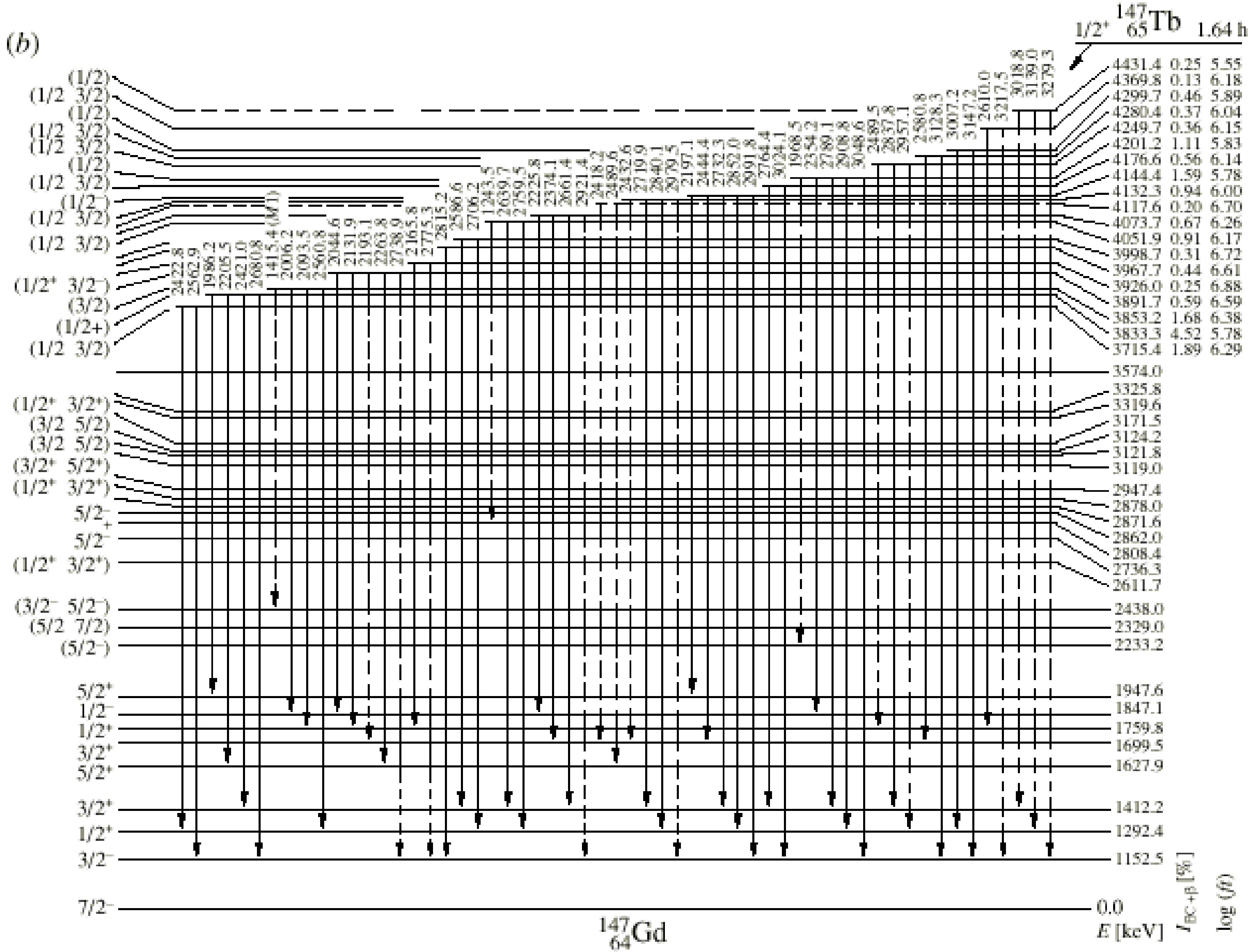

(b)
1/2+ $^{147}_{65}$Tb 1.64 h
$^{147}_{64}$Gd
E [keV]
$I_{EC+\beta}$ [%]
log (ft)
4431.4 0.25 5.55
4369.8 0.13 6.18
4299.7 0.46 5.89
4280.4 0.37 6.04
4249.7 0.36 6.15
4201.2 1.11 5.83
4176.6 0.56 6.14
4144.4 1.59 5.78
4132.3 0.94 6.00
4117.6 0.20 6.70
4073.7 0.67 6.26
4051.9 0.91 6.17
3998.7 0.31 6.72
3967.7 0.44 6.61
3926.0 0.25 6.88
3891.7 0.59 6.59
3853.2 1.68 6.38
3833.3 4.52 5.78
3715.4 1.89 6.29
3574.0
3325.8
3319.6
3171.5
3124.2
3121.8
3119.0
2947.4
2878.0
2871.6
2862.0
2808.4
2736.3
2611.7
2438.0
2329.0
2233.2
1947.6
1847.1
1759.8
1699.5
1627.9
1412.2
1292.4
1152.5
0.0
(1/2)
(1/2 3/2)
(1/2)
(1/2 3/2)
(1/2 3/2)
(1/2)
(1/2 3/2)
(1/2−)
(1/2 3/2)
(1/2 3/2)
(1/2+ 3/2−)
(3/2)
(1/2+)
(1/2 3/2)
(1/2+ 3/2+)
(3/2 5/2)
(3/2 5/2)
(3/2+ 5/2+)
(1/2+ 3/2+)
5/2−
+
5/2−
(1/2+ 3/2+)
(3/2− 5/2−)
(5/2 7/2)
(5/2−)
5/2+
1/2−
1/2+
3/2+
5/2+
3/2+
1/2+
3/2−
7/2−

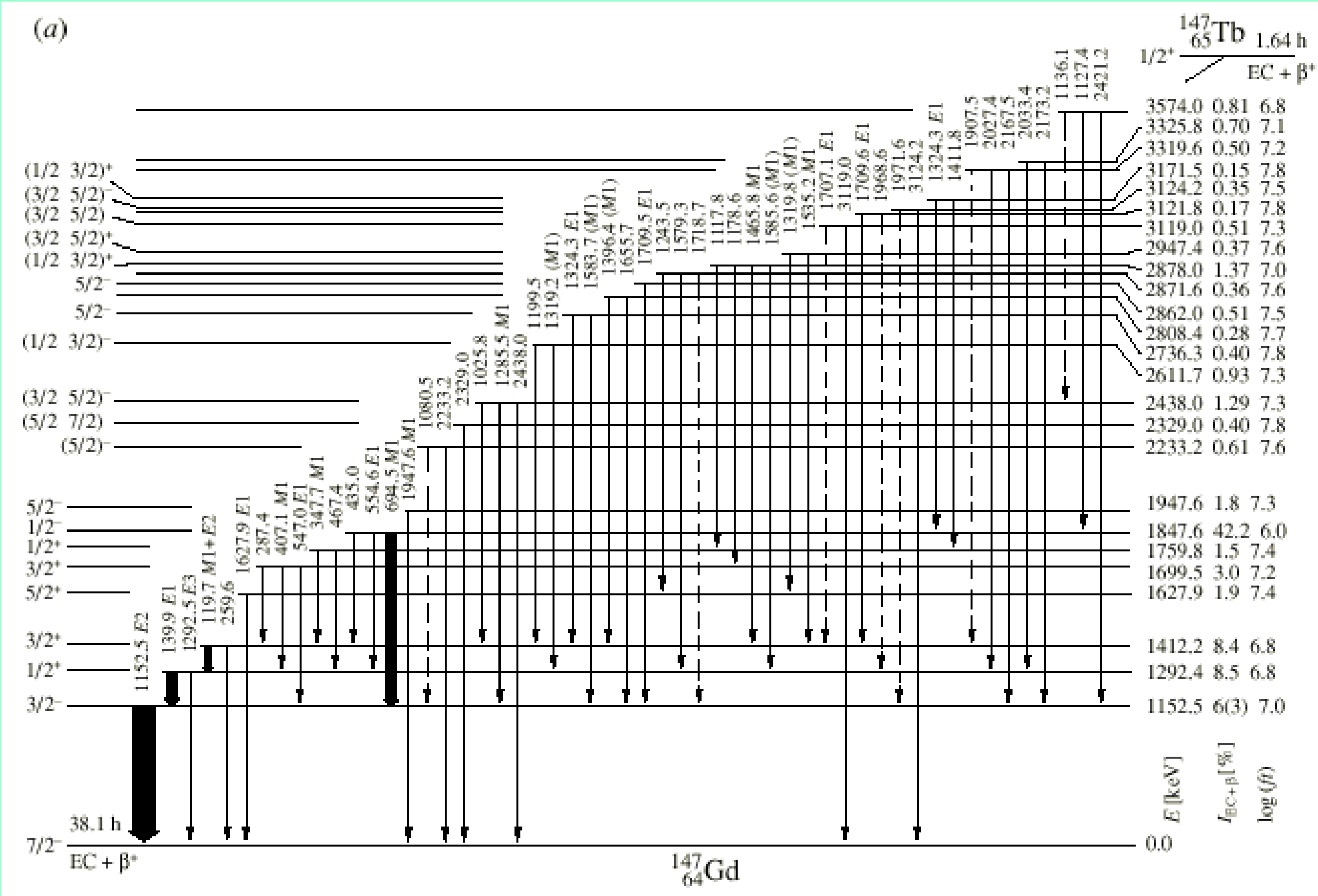
(a)
147 65 Tb 1.64 h
1/2+
EC + β+
1136.1
1127.4
2421.2
1907.5
2027.4
2167.5
2033.4
2173.2
1324.3 E1
1411.8
1707.1 E1
3119.0
1709.6 E1
1968.5
1971.6
3124.2
1117.8
1178.6
1465.8 M1
1585.6 (M1)
1319.8 (M1)
1535.2 M1
1199.5
1319.2 (M1)
1324.3 E1
1583.7 (M1)
1396.4 (M1)
1655.7
1709.5 E1
1243.5
1579.3
1718.7
1080.5
2233.2
2329.0
1025.8
1285.5 M1
2438.0
1947.6 M1
694.5 M1
554.6 E1
435.0
467.4
347.7 M1
547.0 E1
407.1 M1
287.4
1627.9 E1
259.6
119.7 M1+E2
1292.5 E3
139.9 E1
1152.5 E2
(1/2 3/2)+
(3/2 5/2)−
(3/2 5/2)
(3/2 5/2)+
(1/2 3/2)+
5/2−
5/2−
(1/2 3/2)−
(3/2 5/2)−
(5/2 7/2)
(5/2)−
5/2−
1/2−
1/2+
3/2+
5/2+
3/2+
1/2+
3/2−
7/2−
38.1 h
EC + β+
3574.0 0.81 6.8
3325.8 0.70 7.1
3319.6 0.50 7.2
3171.5 0.15 7.8
3124.2 0.35 7.5
3121.8 0.17 7.8
3119.0 0.51 7.3
2947.4 0.37 7.6
2878.0 1.37 7.0
2871.6 0.36 7.6
2862.0 0.51 7.5
2808.4 0.28 7.7
2736.3 0.40 7.8
2611.7 0.93 7.3
2438.0 1.29 7.3
2329.0 0.40 7.8
2233.2 0.61 7.6
1947.6 1.8 7.3
1847.6 42.2 6.0
1759.8 1.5 7.4
1699.5 3.0 7.2
1627.9 1.9 7.4
1412.2 8.4 6.8
1292.4 8.5 6.8
1152.5 6(3) 7.0
0.0
E [keV]
I EC+β [%]
log (ft)
147 64 Gd

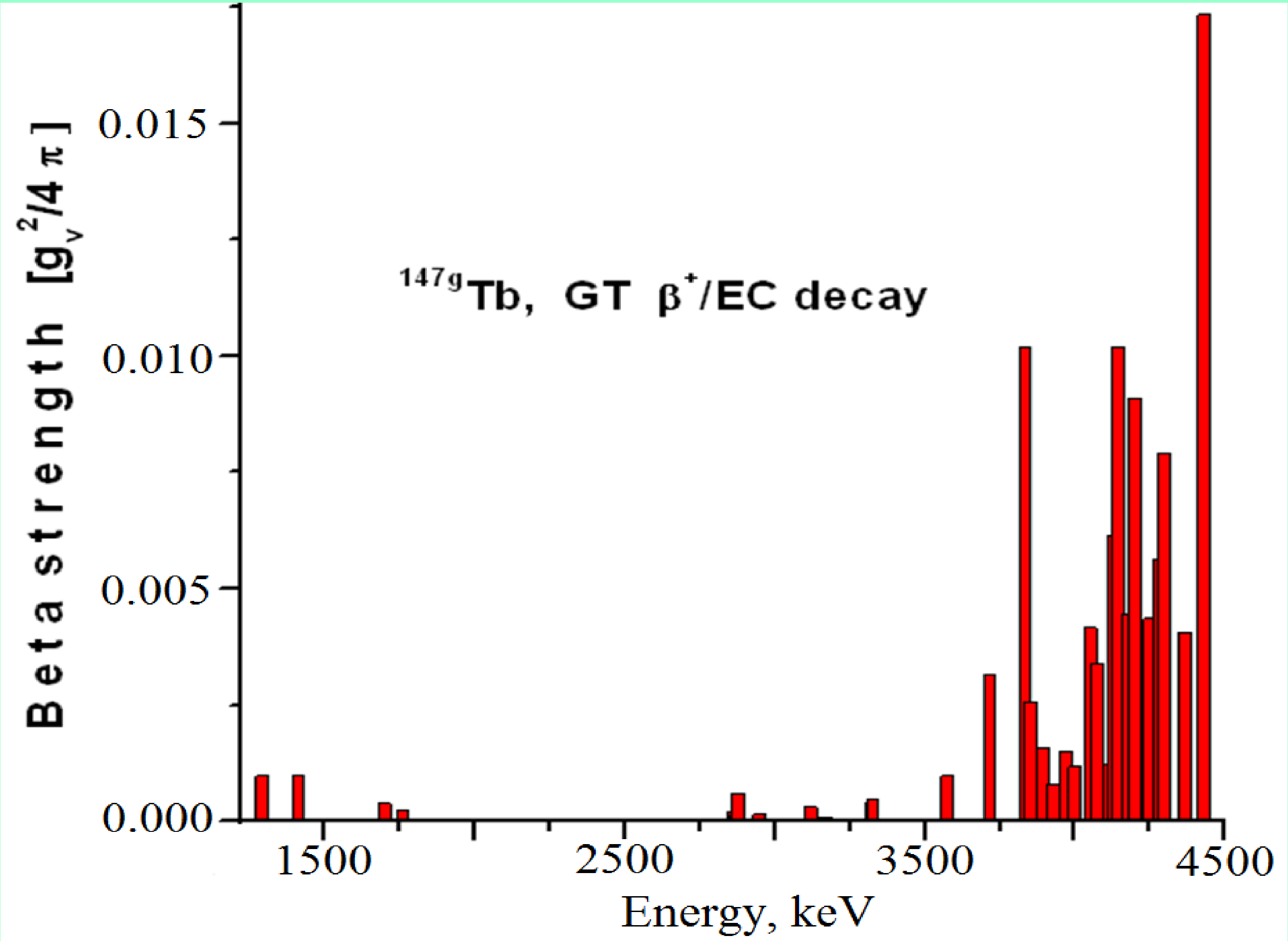

$S_\beta(E)$ for GT transitions in the β+/EC decay of the spherical nucleus ^{147g}Tb ($1/2^+$; $T_{1/2}$ = 1.6 h, Q_{EC} = 4.6 MeV).

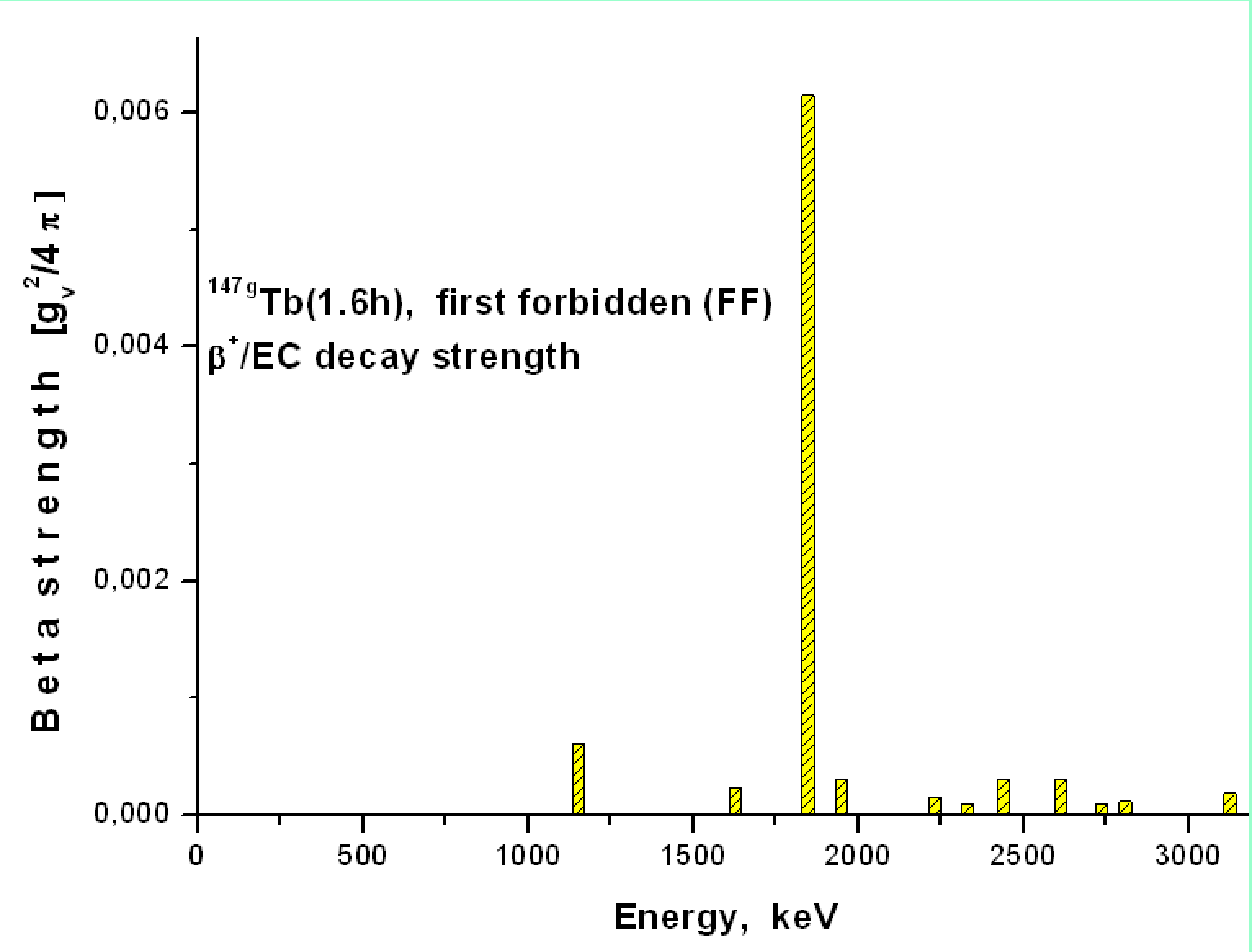

$S_\beta(E)$ for first-forbidden transitions in the β+/EC decay of the spherical nucleus ^{147g}Tb ($T_{1/2}$ = 1.6 h, Q_{EC} = 4.6 MeV).

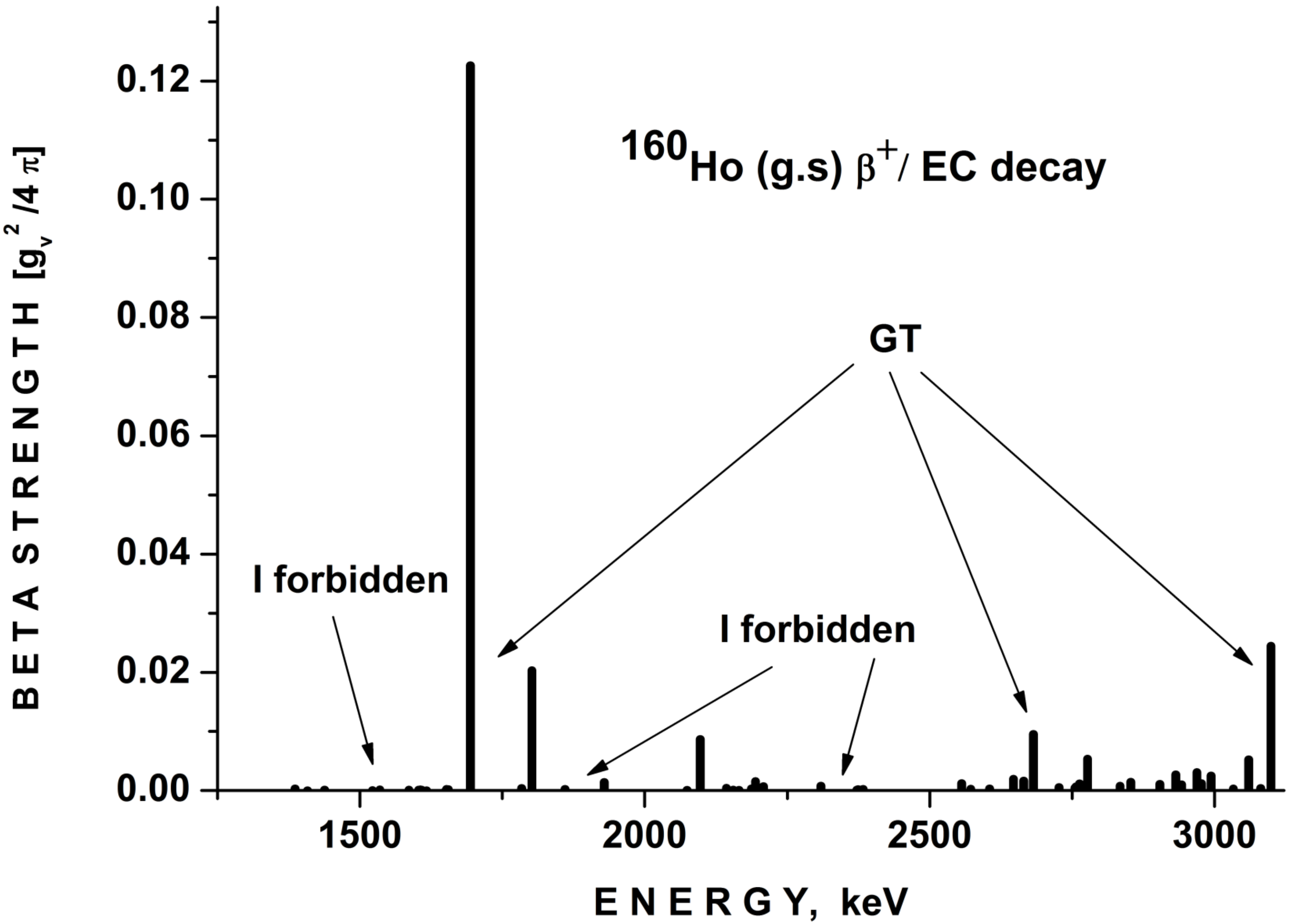

^{160}Ho (g.s) β^+/ EC decay
GT
I forbidden
I forbidden
B E T A S T R E N G T H [g_v^2 /4 π]
E N E R G Y, keV
0.00
0.02
0.04
0.06
0.08
0.10
0.12
1500
2000
2500
3000

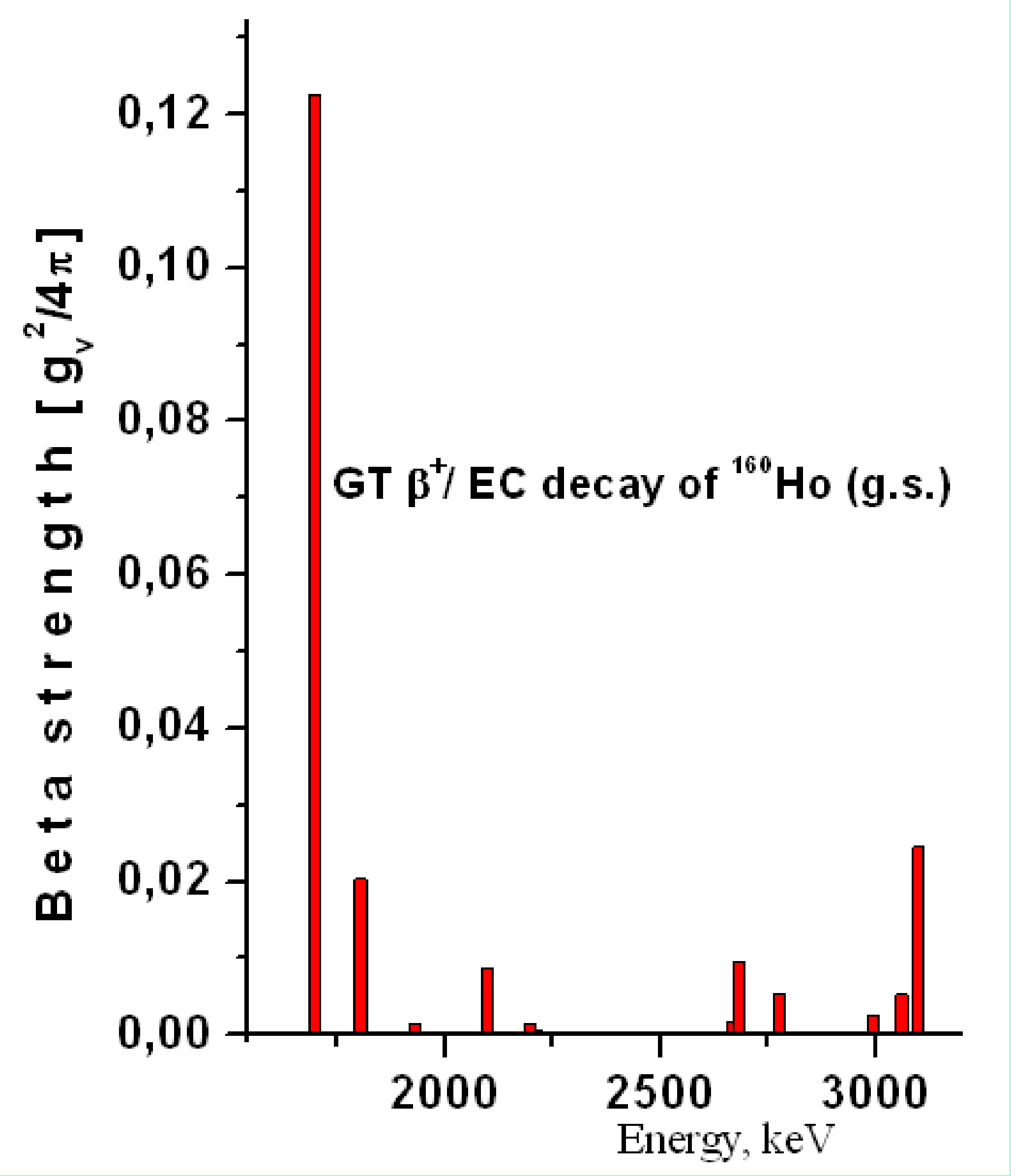

$S_\beta(E)$ for Gamow–Teller transitions in the β+/EC decay of the deformed nucleus ^{160g}Ho (5^+ ;25.6 min), Q_{EC} = 3286(15) keV.

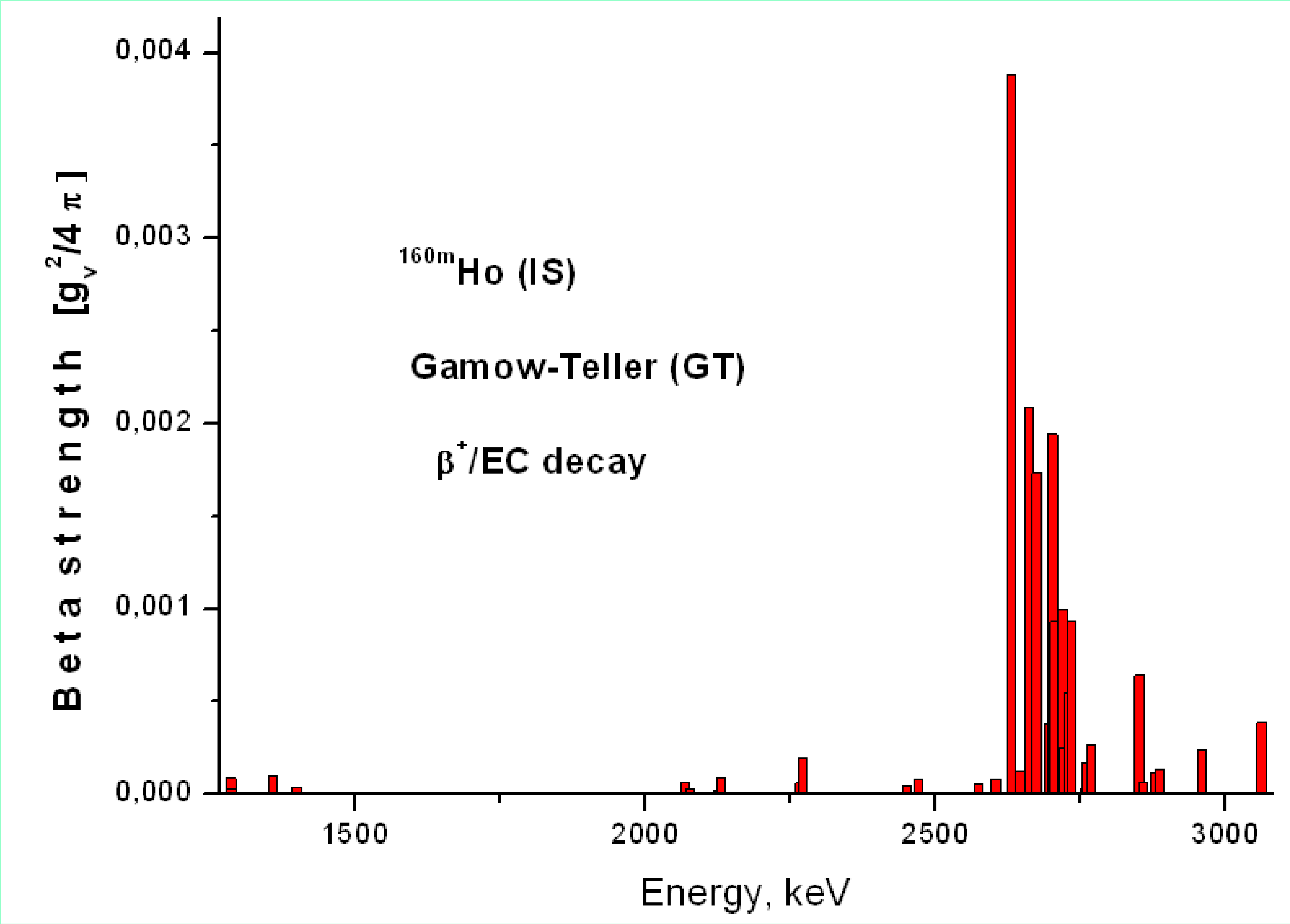

$S_\beta(E)$ for Gamow–Teller transitions in the β+/EC decay of the deformed nucleus of the isomer ^{160m}Ho (2^-; 5.02 h), Q_{EC} = 3346 keV

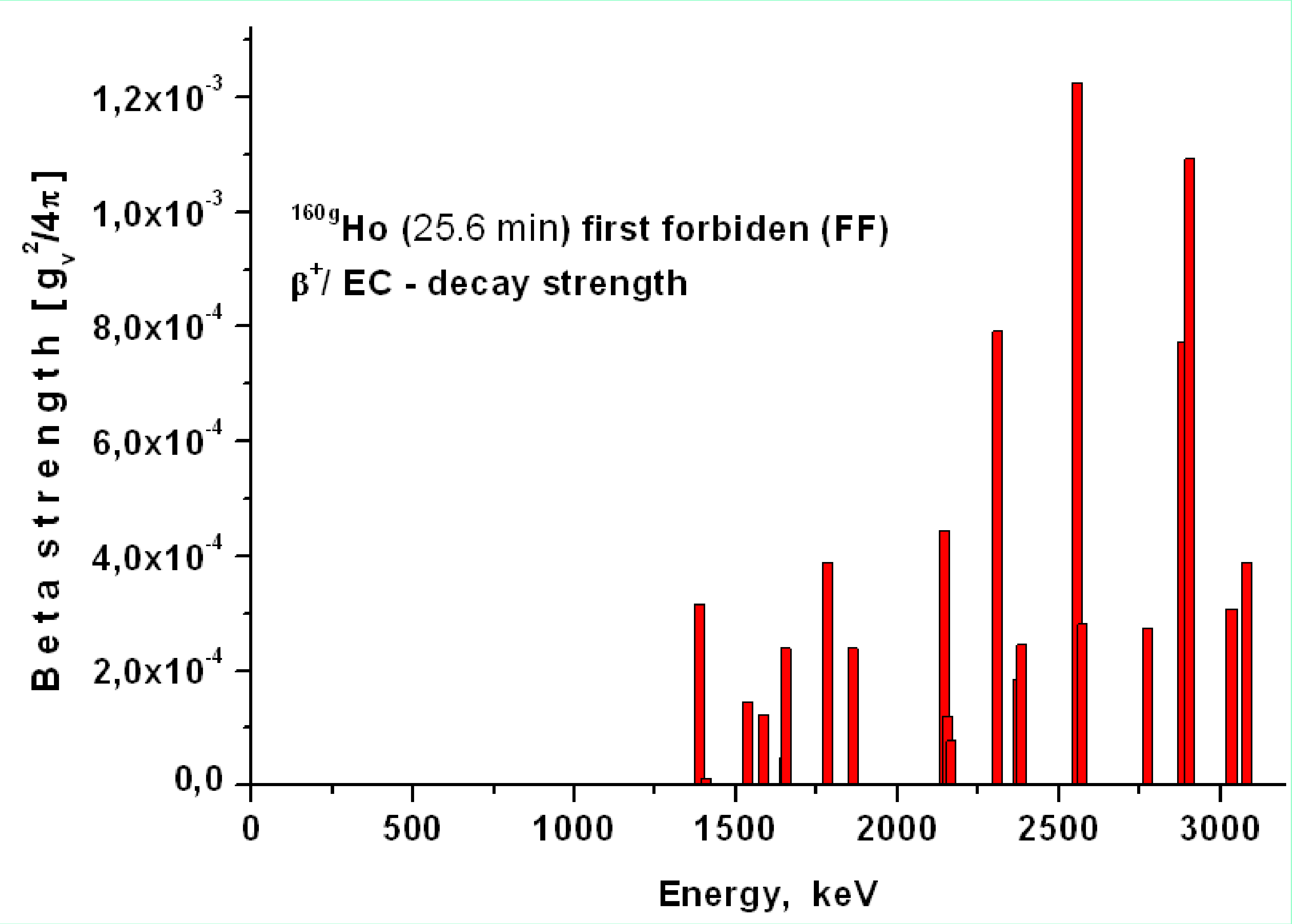

$S_{\beta}(E)$ for Gamow–Teller transitions in the β+/EC decay of the deformed nucleus of the isomer ^{160m}Ho (2^-; 5.02 h), Q_{EC} = 3346 keV

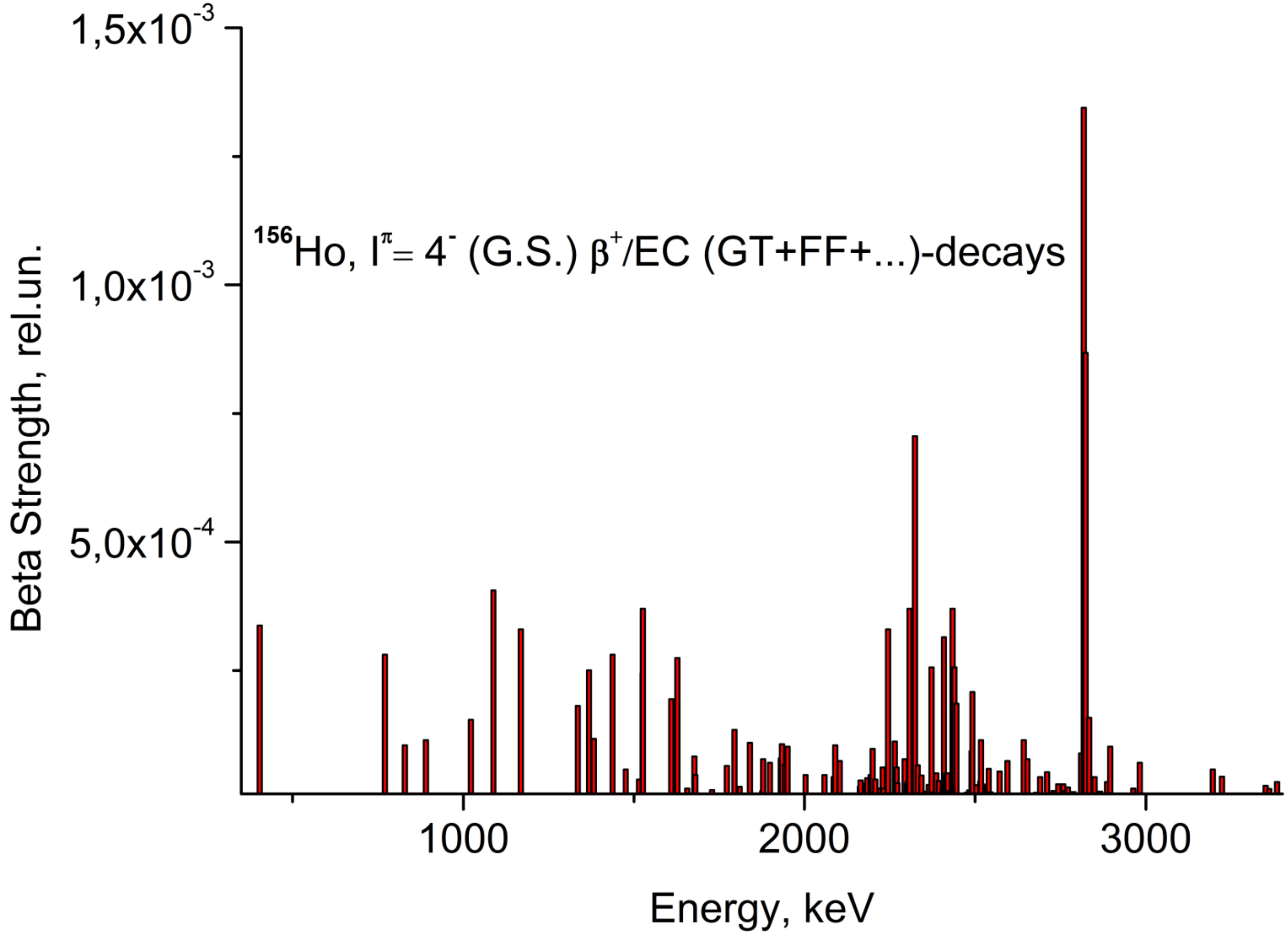

1,5x10^-3
1,0x10^-3
5,0x10^-4
Beta Strength, rel.un.
156Ho, Iπ = 4- (G.S.) β+/EC (GT+FF+...)-decays
1000
2000
3000
Energy, keV

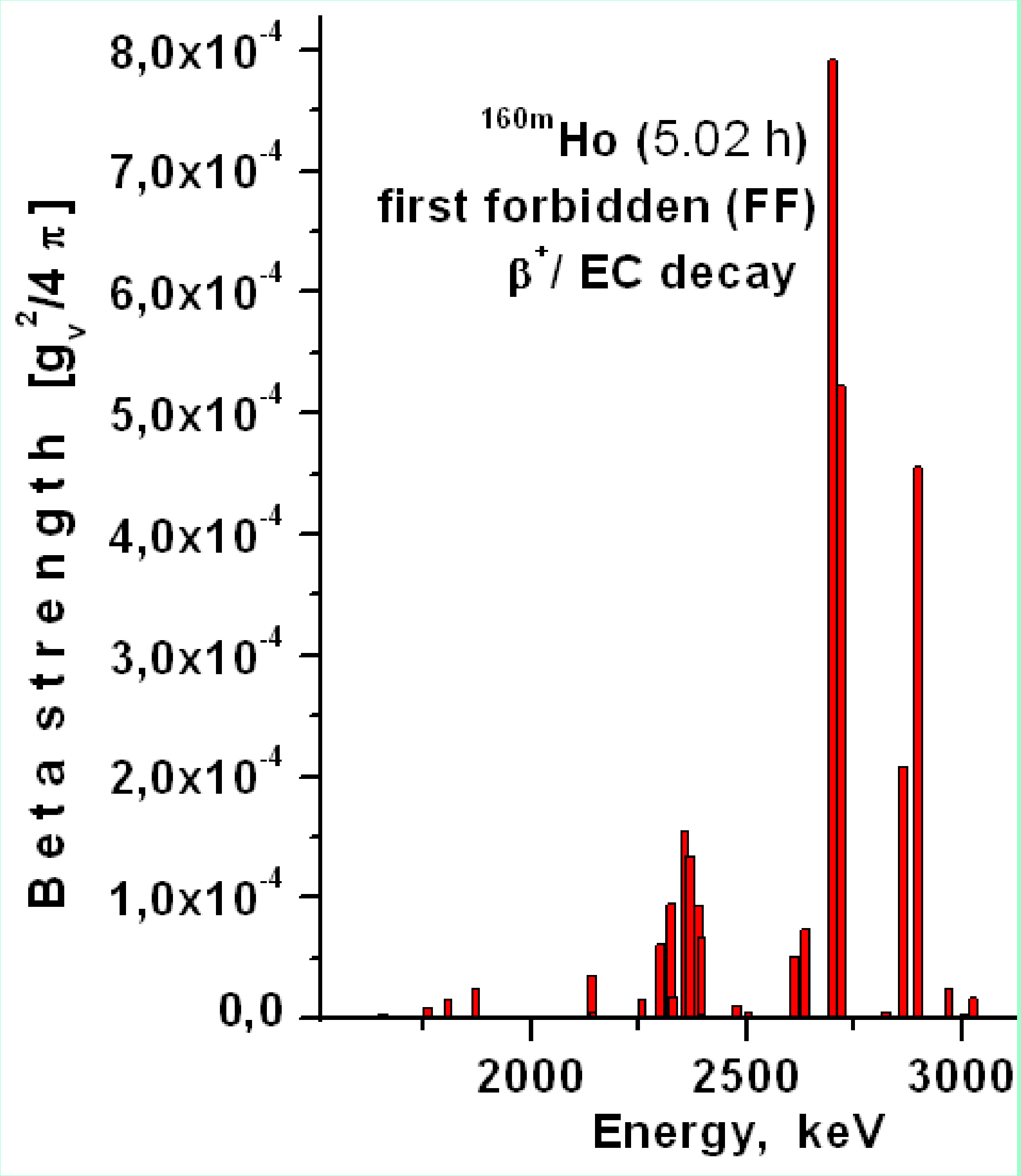

$S_\beta(E)$ for first-forbidden transitions in the β+/EC decay of the deformed nucleus of the isomer ^{160m}Ho (5.02 h)

Bohr A., Mottelson B. // Nuclear Structure V. 1. 1969. Benjamin, New York

$B^{\pm}(\mathrm{GT},E)=((g^{eff}_A)^2/4\pi)\,|\langle I_f \| \sum t_{\pm}(k)\sigma(k) \| I_i\rangle|^2/(2I_i+1),$ (1)

$B^{\pm}(\mathrm{GT},E) = [D(g^2_V/4\pi)]/ft,\ D = (6144 \pm 2)$ sec (2)

$S^- - S^+ = 3(N-Z)$, (Ikeda sum rule) (3)

$S^{\pm} = \Sigma_f |\langle I_f \| \sum t_{\pm}(k)\,\sigma(k) \| I_i\rangle|^2/(2I_i+1),$ (4)

$\sum_j B^-(\mathrm{GT},E_j) - \sum_k B^+(\mathrm{GT},E_k) = 3(N-Z)(g^{eff}_A)^2/4\pi,$ (5)

Naumov Yu.V., Bykov A.A., Izosimov I.N. Structure of β-decay strength functions // Sov. J. Part. Nucl. 1983. V.14, No 2. P.175.

$d(I(E))/dE = S_\beta(E)\, T_{1/2}\, f(Q_\beta - E),$ (6)

$(T_{1/2})^{-1} = \int S_\beta(E) f(Q_\beta - E)\, dE,$ (7)

$\int_{\Delta E} S_\beta(E)dE = \sum_{\Delta E} 1/(ft),$ (8)

where $S_\beta(E)$ is in units Mev^{-1} s^{-1}, and *ft* is in seconds.

$\sum_j D/ft_j = 3(N-Z)\,(g^{eff}_A/g_V)^2$ (Ikeda sume rule if ALL GT strength is in Q_β window) (9)

Instead of $B^{\pm}$(GT,E) (usually given in units of ($(g^{eff}_A)^2/4\pi$) or in ($g^2_V/4\pi$), and ($g^2_A/4\pi$),) the quantities $B(\mathrm{GT},E)=|\langle I_f \| \sum t_{\pm}(k)\sigma(k) \| I_i\rangle|^2/(2I_i+1)$ and $B'(\mathrm{GT},E)=4\pi/\, g^2_A\, B(\mathrm{GT},E)$ are often used in the literature.

Some times there are errors in due to not proper using $B^{\pm}$(GT,E), B'(GT,E), and B(GT,E).

The test of error absent is : in ALL cases one must obtain the formula: $\sum_j D/ft_j = 3(N-Z)\,(g^{eff}_A/g_V)^2$ (Ikeda sume rule if ALL GT strength is in Q_β window)

Determination of g_V. For g_V determination it is necessary to have the total strength of the Fermi β-transitions in the energy window allowed for beta decay. According to the isospin selection rule, the only state which can be reached by the Fermi beta transition is the isobar-analogue resonance IAR and model independent relation (Sum rule) for β-transitions between Isobar Analog States (IAS) $TM_T \rightarrow TM_{T\pm1}$ is:

$$[T\,(-/+)\,M_T][T \pm M_T + 1] = [(2\pi^3\hbar^7 \ln 2)/(\mathbf{g_V}^2 m_e^5 c^4)]/\boldsymbol{ft}$$

Only some nuclei (i> = ${}^{10}_{6}C$, ${}^{14}_{8}O$, ${}^{26m}_{13}Al$, ${}^{34}_{17}Cl$, ${}^{42}_{21}Sc$, ${}^{46}_{23}V$, ${}^{50}_{25}Mn$, ${}^{54}_{27}Co$)

are known where IAS is in Q_β window and pure Fermi transitions ($0^+ \rightarrow 0^+$) take place.

Constant D (and g_V) was determined experimentally.

$$D \equiv [(2\pi^3\hbar^7 \ln 2)/(\mathbf{g_V}^2 m_e^5 c^4)] = (6144 \pm 2)\ \text{sec}$$

Usualy $g^2{}_V/4\pi$ use as a "unit", i.e. experimental B(GT) presented in $g^2{}_V/4\pi$ units, sometimes in $g^2{}_A/4\pi$ units, where for neutron beta decay: $(g_A/g_V)^2 = 1.618 \pm 0.006$.

The **conserved vector-current hypothesis (CVC) and partially conserved axial-vector-current hypothesis (PCAC)** yield the free-nucleon value, determined **from neutron beta decay is g_A^{free}/g_V = -1.2723(23)**. **Inside nuclear** matter the **effective value g_A^{eff} is needed** to reproduce experimental observations.

Precise **information on the value of g_A^{eff} is crucial** when predicting half-life for beta decays, beta decay strength function for Gamow-Teller (GT) and first forbidden (FF) beta transitions, and cross section for charge-exchange reactions. The effective value of g_A^{eff} is characterized by a renormalization factor q (in the case of quenching of g_A it is called "quenching factor"): $q=g_A^{eff}/g_A^{free}$, where g_A^{eff} is the value of the axial-vector coupling derived from a given theoretical or experimental analysis.

The **origin of the quenching of the g_A value is not completely known** and various mechanisms have been proposed for its origin including tensor effects, the Δ-isobar admixture to the nuclear wave function, relativistic corrections to the Gamow-Teller operator, etc., but a clean separation of these aspects is difficult.

Determination of g^{eff}_A.

1. **Model depended** determination from experimental *ft* valuas.
$B^{\pm}(GT,E)=((g^{eff}_A)^2/4\pi)|\langle I_f\|\sum t_{\pm}(k)\sigma(k)\|I_i\rangle|^2/(2I_i+1)$,
$B^{\pm}(GT,E) = [D(g^2_V/4\pi)]/ft$. $|\langle I_f\|\sum t_{\pm}(k)\sigma(k)\|I_i\rangle|^2$ - calculated in different models, *ft* – from experiment → $(g^{eff}_A/g_V)^2$ extracted.

2. **Model independed** determination. **Ikeda sum rule** – comparison of the experimental total GT beta decay strength with the Ikeda sum rule is **the model independed metod**. For application of this method it is necessary to **have the total GT strength** in the energy window allowed for beta decay, and contribution from non-nucleonic degries of freedom (Δ-isobar, for example) must be neglectable. **Such situation may be realized for beta decay of halo nuclei (^{6}He, ^{11}Li, …) or for very neutron-rich nuclei where, $E_{GTR} < E_{IAR}$.**

For $|$**N-Z**$|$ **» 0** nuclei the **maximum excitation energy** corresponds to the main resonance in $S_\beta(E)$. Other, more weak resonances (pygmy resonances) have smaller excitation energies. Such type of $S_\beta(E)$ take place for ^{11}Be. **Shell-model results is that the GTR energy can be lower than the IAS energy**, i.e. E(GT) – E(IAS) < 0 **for very neutron-rich nuclei**. For ^{11}Be: $E_{GTR} < E_{IAR}$, $E_{GTR} - E_{IAR} = -2.97$ MeV.

For **N≈Z** nuclei structure of $S_\beta(E)$ may have opposite type, i.e. **the minimum excitation energy** corresponds to the main resonance in $S_\beta(E)$ [low-energy super-Gamow-Teller phonon or GTR]. Such type of S_β(E) take place for ^{6}Li. For ^{6}Li: $E_{GTR} < E_{IAR}$, $E_{GTR} - E_{IAR} = -3562.88$ keV.

We shall accept a state as a quantum halo if the two conditions are fulfilled, i.e., there is a sufficiently large cluster configuration with a sufficiently large spatial extension.

The accepted definition of a halo nucleus (typically in its ground state) is therefore that the halo nucleon is required to have more than 50% of its probability density outside the range of the core potential.

Halo states require low relative angular momentum (centrifugal barrier) for the valence particle (L=0,1 for 1n or 1p halo), as well as weak binding.

Centrifugal barrier prevents for halo formation

Coulomb barrier prevents for proton halo formation.

High level density of nonhalolike levels prevents halo formation in excited states

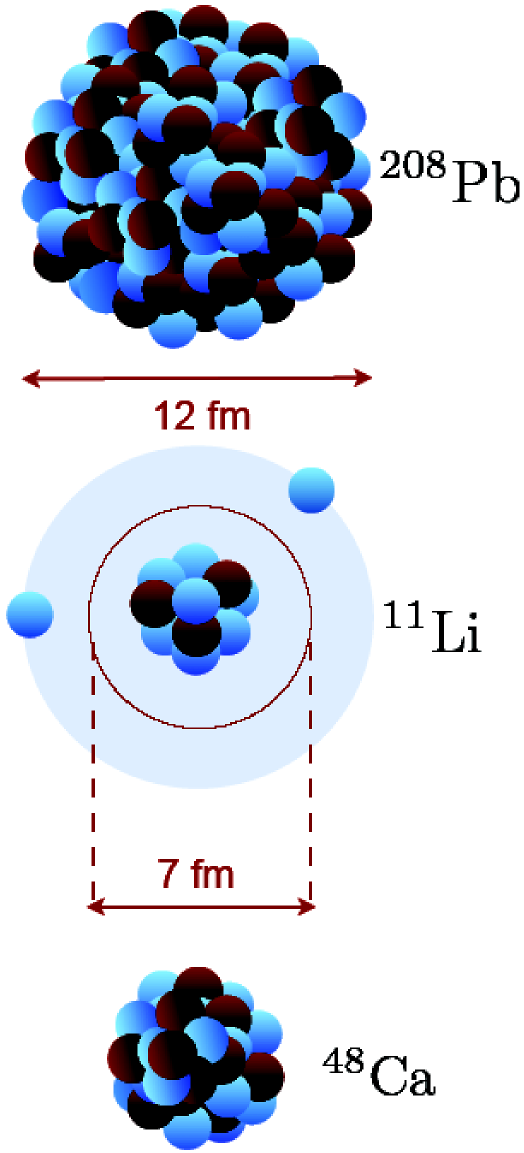

Nuclear radius for stable nuclei: $R_N \sim r_0 A^{1/3}$ with $r_0 \sim 1.2$ fm

strongly clusterised system:
neutrons tunnel far from the core
and form a halo

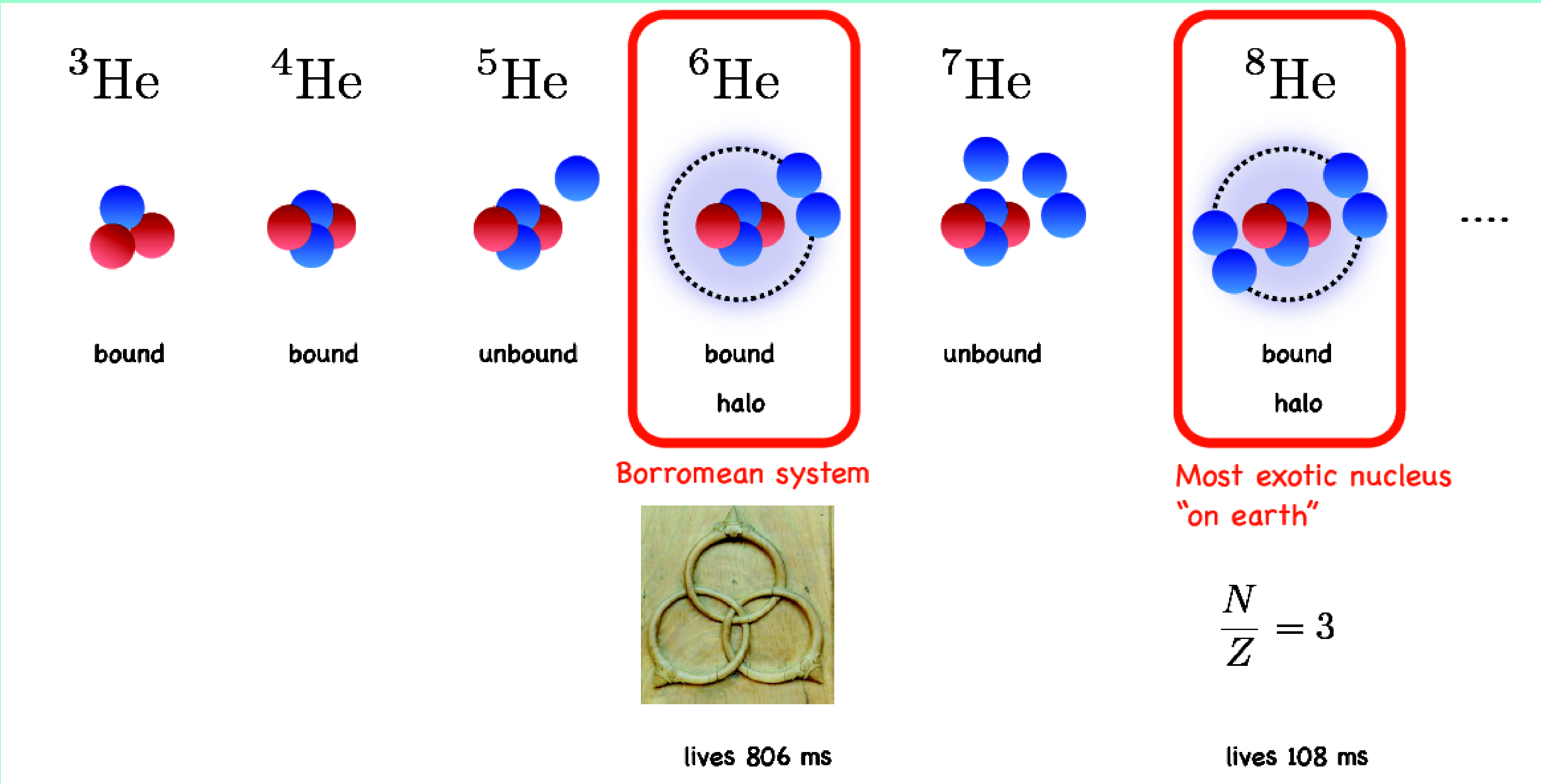
^{3}He
^{4}He
^{5}He
^{6}He
^{7}He
^{8}He
....
bound
bound
unbound
bound
halo
unbound
bound
halo
Borromean system
Most exotic nucleus
"on earth"
$\frac{N}{Z} = 3$
lives 806 ms
lives 108 ms

In **Borromean** systems the two-body correlations are too weak to bind any pair of particles while the three-body correlations are responsible for the system binding as a whole. In states with one and only one bound subsystem the bound particles moved in phase and were therefor named **“tango states”**

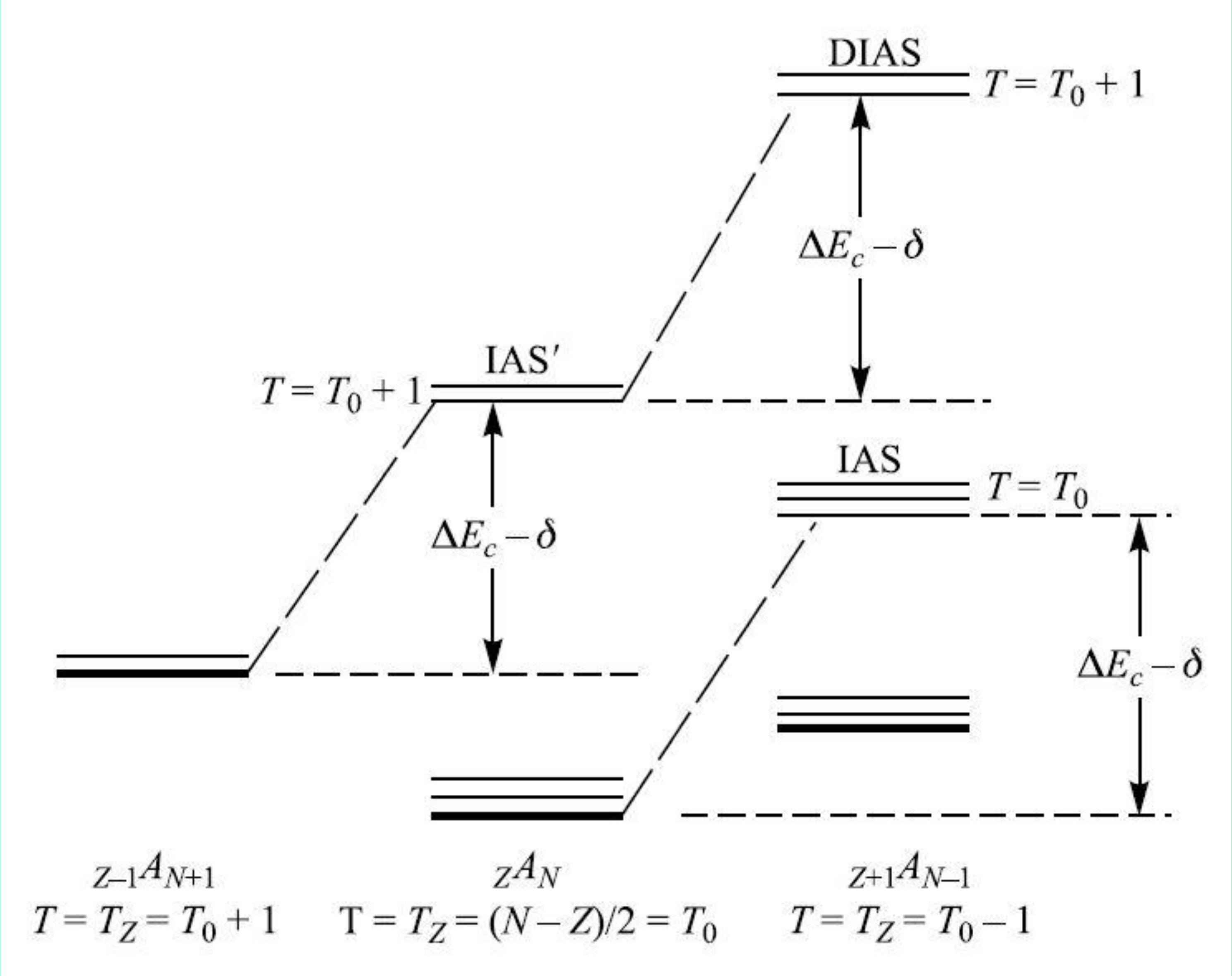

DIAS
$T = T_0 + 1$
$\Delta E_c - \delta$
IAS′
$T = T_0 + 1$
$\Delta E_c - \delta$
IAS
$T = T_0$
$\Delta E_c - \delta$
${}_{Z-1}A_{N+1}$
$T = T_Z = T_0 + 1$
${}_{Z}A_{N}$
$\mathrm{T} = T_Z = (N - Z)/2 = T_0$
${}_{Z+1}A_{N-1}$
$T = T_Z = T_0 - 1$

In the general case the **IAS is the coherent superposition of the excitations like neutron hole–proton particle coupled to form the momentum J = 0^+.** The IAS has the isospin $T=T_z+1=(N-Z)/2+1$, where $T_z = (N - Z)/2$ is the isospin projection. The isospin of the ground state is $T = T_z = (N - Z)/2$. When the IAS energy corresponds to the continuum, the IAS can be observed as a resonance. **Configuration states (CS) are not the coherent superposition of such excitations** and have $T = T_z = (N - Z)/2$. One of the best studied CS is the anti-analog state (AIAS). The CS formation may be restricted by the Pauli principle. The Double Isobar Analog State (DIAS) has the isospin $T = T_z + 2$ and is formed as the coherent superposition of the excitations like two neutron holes–two proton particles coupled to form the momentum $J = 0^+$.

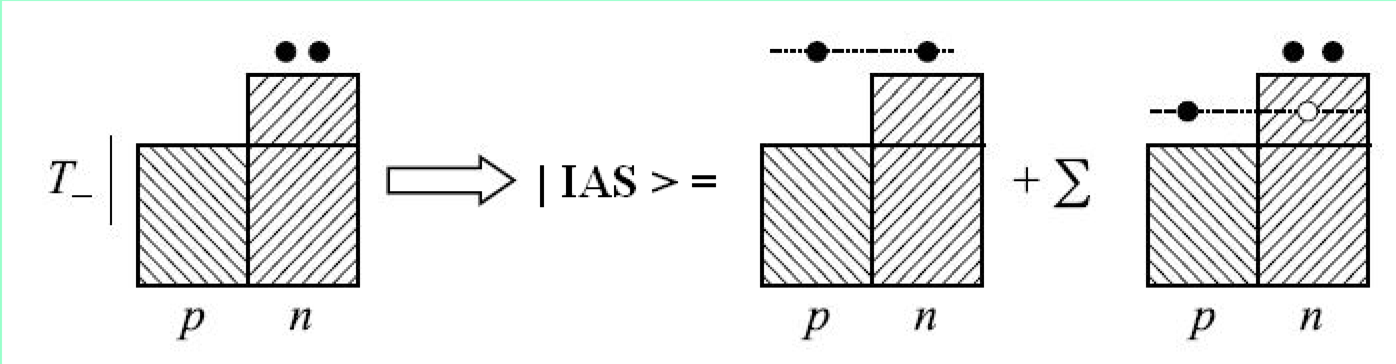

T_
| IAS > =
+ Σ
p n
p n
p n

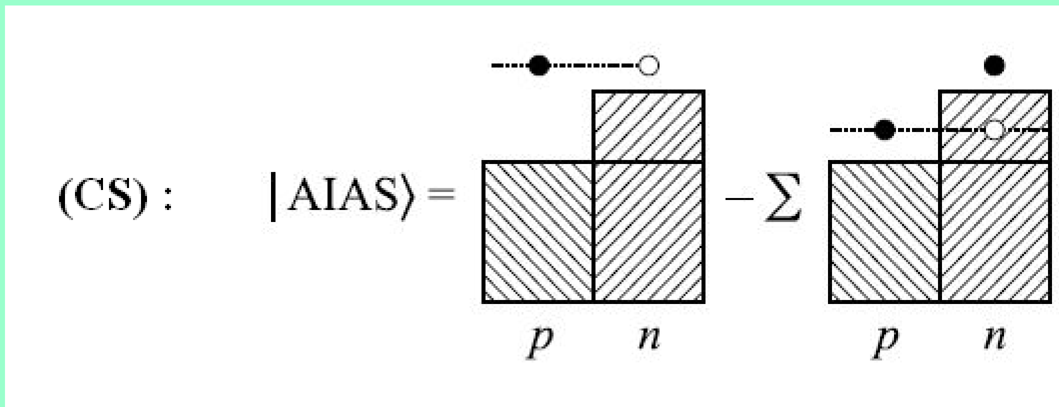

(CS) :
|AIAS⟩ =
– Σ
p n
p n

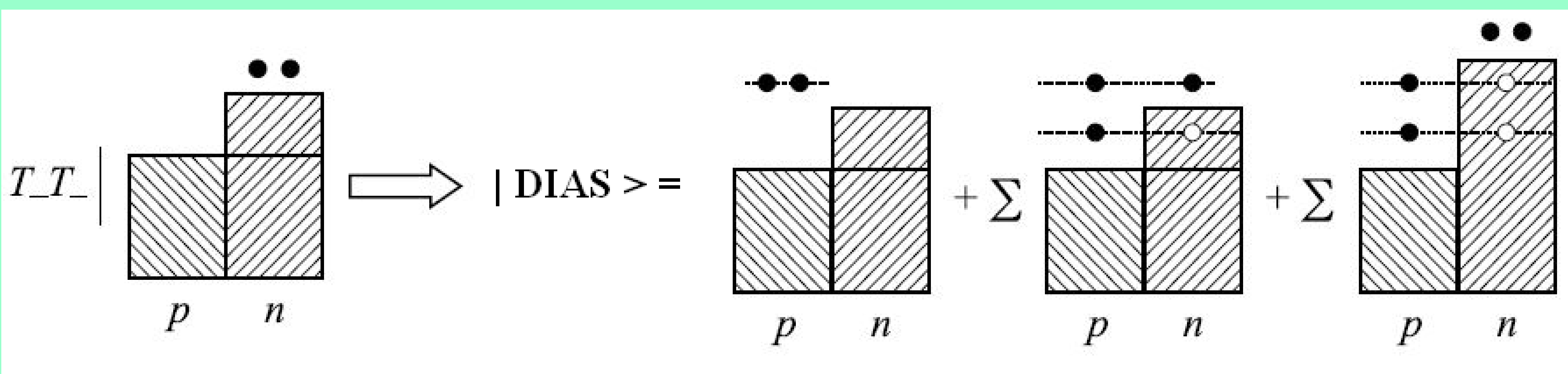

T_T_
| DIAS > =
+ Σ
+ Σ
p n
p n
p n
p n

Since the operators of GT β-decay and *M*1 γ-decay have no spatial components (the radial factor in the *M*λ *γ*-transition operator is proportional to $r^{\lambda-1}$), GT β-transitions and *M*1 γ-transitions between states **with similar spatial shapes are favored.**

For the GT β-transitions essential configurations include states made up of the ground state of parent nucleus by the action of the Gamow-Teller operator of the β-transition $\boldsymbol{Y}_- = \sum \boldsymbol{\tau}(\boldsymbol{i})_-\boldsymbol{\sigma}_m(\boldsymbol{i})$, where $\boldsymbol{\tau}_-(\boldsymbol{i})\boldsymbol{\sigma}_m(\boldsymbol{i})$ – spin-isospin operator.

Let us take as the parent state the wave function for the ground state of the nucleus in which two neutrons make up the nuclear Borromean halo (*nn* halo) and act on it by the operator $\boldsymbol{Y}_-$

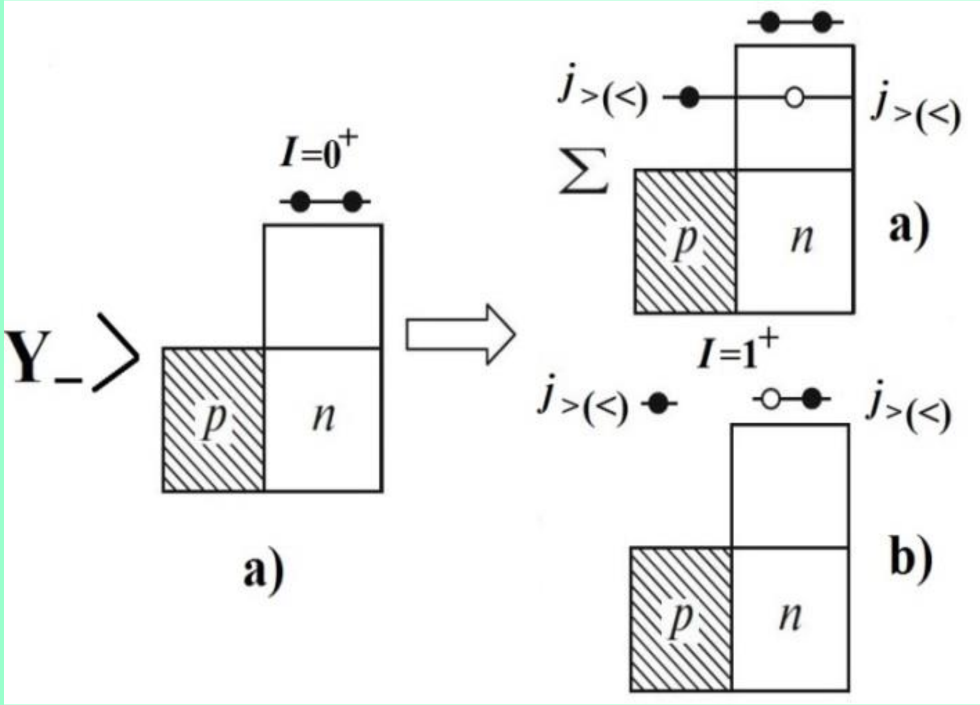

Proton particle–neutron hole coupled to form the spin-parity $I^{\pi} = 1^{+}$ and core polarization (CP) states: **a) *nn* Borromean halo** component, **b) *np* tango halo** component.

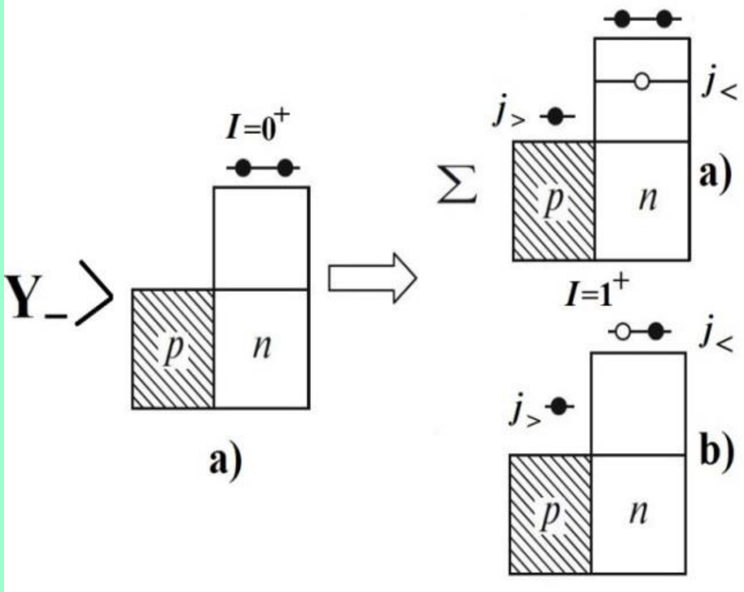

Proton particle–neutron hole coupled to form the spin-parity $I^\pi = 1^+$ and back spin flip (BSF) states: a) *nn* Borromean halo component, b) *np* tango halo component.

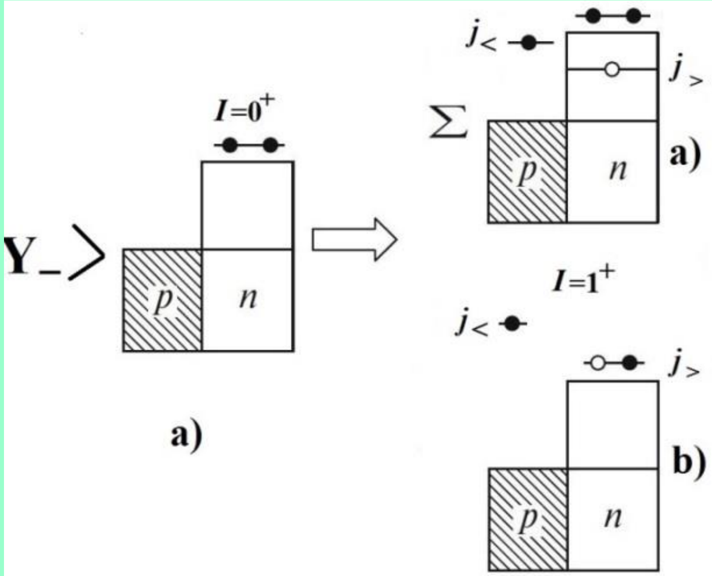

Proton particle–neutron hole coupled to form the spin-parity $I^\pi = 1^+$ and spin flip (SF) states: a) *nn* Borromean halo component, b) *np* tango halo component.

Coherent superposition of CP, BSF, and SF configurations forms **Gamow-Teller (GT) resonance**. **Non coherent superposition** forms resonances in $S_\beta(E)$ at excitation energy E lower than energy of GT resonance (so-called **pygmy resonances**). Beacause after action of ***Y_*** operator on *nn* Borromean halo configuration with I^π=0^+ the ***np* tango halo configurations with I^π=1$^+$** are formed, the GT and pygmy resonances in $S_\beta(E)$ will have components corresponging to *np* tango halo. When neutron excess number is high enough, the SF, CP, and BSF configurations may simultaneously have both *nn* Borromean halo component and *np* tango halo component and form so called mixed halo .

Two neurons that form the *nn* halo in ^{6}He ground state (g.s.) occupy the $1p$ orbit ($p_{3/2}$ configuration with a 7% admixture of $p_{1/2}$ configuration). The remaining two neutrons and two protons occupy the $1s$ orbit. Therefore, the action of the operator $\boldsymbol{T}_{-}$ on the g.s. wave function for the ^{6}He nucleus ($T = 1$, $T_z = 1$) results in the formation of the analogue state with the configuration corresponding to the *pn* halo. This IAR is in the ^{6}Li nucleus ($T = 1$, $T_z = 0$) at the excitation energy 3.56 MeV. The width of this state is $\Gamma = 8.2$ eV, which corresponds to the half-life $T_{1/2} = 6 \cdot 10^{-17}$ s. The theoretical and experimental data indicate that this IAR state has a *np* halo. Formation of configuration states is prohibited by the Pauli principle. **The Isobar Analog State (IAS) of the ^{6}He g.s. (*nn* Borromean halo nucleus), i.e., the 3.56 MeV, $I=0^{+}$ state of ^{6}Li, has a *np* halo structure of Borromean type.**

Since the operators of GT β-decay and *M*1 γ-decay have no spatial components (the radial factor in the *M*λ *γ*-transition operator is proportional to $r^{\lambda-1}$), GT β- and *M*1 γ-transitions between states with similar spatial shapes are favored.

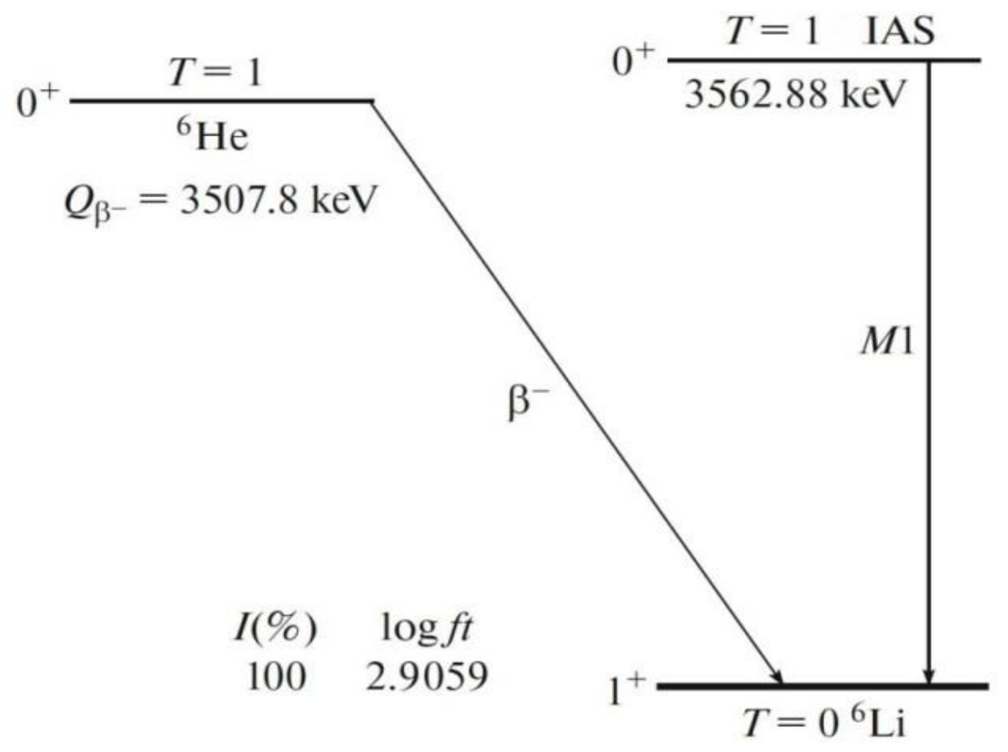

. Connection between the *ft* value for *β*-decay of the parent state (^{6}He g.s.) and the B(*M*1,σ) value for γ-decay of the IAS (^{6}Li, E = 3562 keV). $ft = 11633/[T_0 \times B(M1,\sigma)]$, *ft* in sec, T_0-isospin of the parent state, B(*M*1,σ) in μ_0^2 , B(*M*1,σ) = 8.2 W.u., B(*M*1) ≈ 8.6 W.u., for *M*1 γ-transition W.u. = 1.79 μ_0^2.

A rather large value of the reduced probability of *M*1 γ-transition (*B*(*M*1,σ) = 8.2 W.u.) for *M*1 γ-decay from IAS and large *B*(GT) = 7.630$g_V^2/4\pi$ (Σ(Ikeda sum rule) = 6$g_A^2/4\pi$) value for β^--transition to the ground state is evidence for the existence of tango halo structure in the ^{6}Li ground state.

The IAS in ^{6}Li has the **Borromean *n-p* halo** structure since the *n-p* subsystem is coupled to the spin-parity $I^\pi = 0^+$, i.e. **unbound**, whereas *n-p* subsystem for the ^{6}Li g.s. is coupled to the spin-parity $I^\pi = 1^+$, i.e. **bound**. According to halo classification, such structure of the ^{6}Li g.s. corresponds to the ***n-p* tango halo**.

Because of large B(GT) value (B(GT) = $7.630 g_V^2/4\pi$), the ^{6}Li g.s. has structure corresponding to the low-energy Gamow-Teller phonon and the energy of this GT phonon is lower than ($E_{GT} < E_{IAR}$) the energy of IAR (E_{IAR}= 3562.88 keV). In heavy and middle nuclei, because of repulsive character of the spin-isospin residual interaction, the energy of GT resonance is larger than the energy of IAR ($E_{GT} > E_{IAR}$).

In tango halo nucleus ^{6}Li (g.s.) for low energy GT phonon we have $E_{GT} < E_{IAR}$, $E_{GT} - E_{IAR}$= -3562.88 keV, and (N-Z)/A = 0.33 for ^{6}He (^{6}He g.s. is the parent state). Such situation may be connected with contribution of the attractive component *(Fujita Y., et al.* High-resolution study of Gamow-Teller excitations in the ^{42}Ca(^{3}He,*t*) ^{42}Sc reaction and the observation of a "low-energy super-Gamow-Teller state" // Phys. Rev. C. 2015. V. 91. P. 064316, and references therein) of residual interaction in this nucleus.

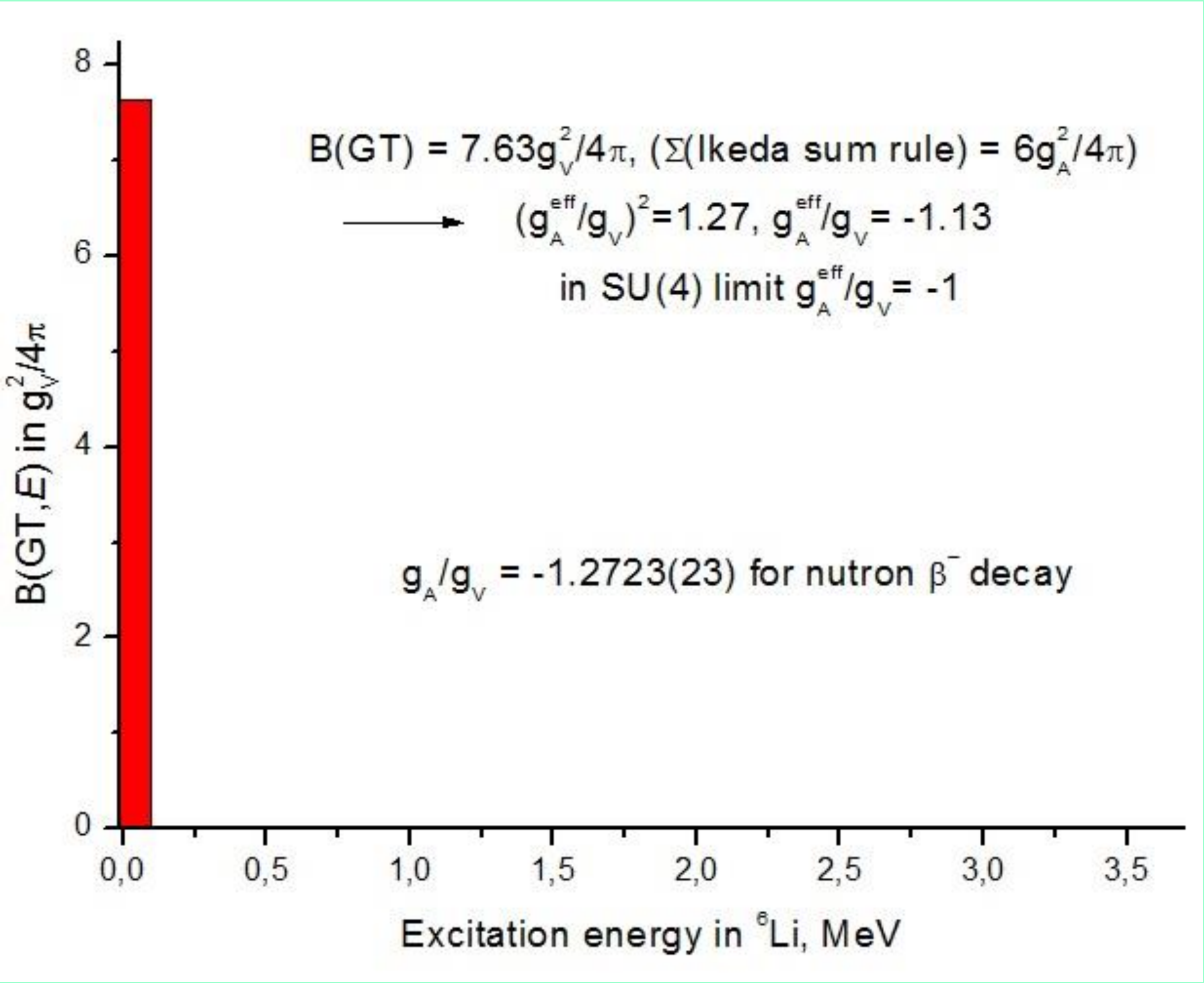

B(GT) = 7.63g$_V^2$/4π, (Σ(Ikeda sum rule) = 6g$_A^2$/4π)
(g$_A^{eff}$/g$_V$)^2=1.27, g$_A^{eff}$/g$_V$= -1.13
in SU(4) limit g$_A^{eff}$/g$_V$= -1
g$_A$/g$_V$ = -1.2723(23) for nutron β$^-$ decay
B(GT,E) in g$_V^2$/4π
Excitation energy in ^{6}Li, MeV
0
2
4
6
8
0,0
0,5
1,0
1,5
2,0
2,5
3,0
3,5

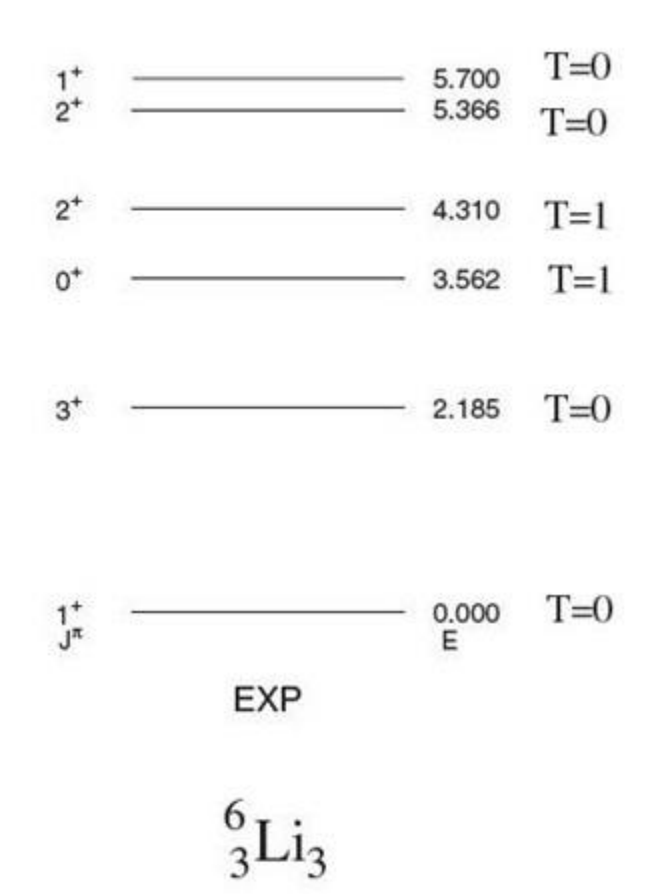

Y. Fujita, Y. Utsuno, H. Fujita
Properties of Low-energy Super Gamow-Teller State, JPS Conf. Proc. **23**, 012030 (2018)

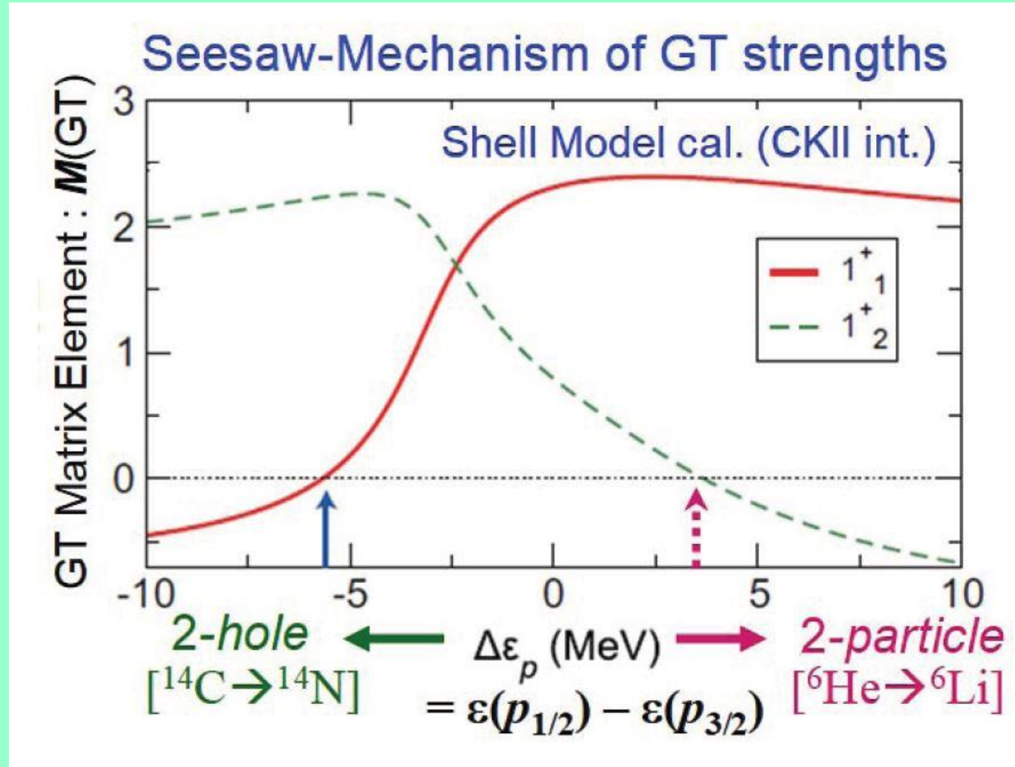

$\Delta\varepsilon_{ls} \approx 1.4\ V_{ls}\ (\mathbf{l}\cdot\mathbf{s})\ A^{-2/3}$, $\Delta\varepsilon_{ls}(p_{1/2}-p_{3/2}) \approx 6$ MeV for ^{6}Li

→ $M(GT)1_2^+/M(GT)_{tot} \leq 0.1$ → $B(GT)\ 1_2^+/B(GT)_{tot} \leq 0.01$ for ^{6}Li, $E(1_2^+) = 5.7$ MeV,

$(g_A^{eff}/g_V)^2 = 1.272 \pm 0.010$, without $B(GT)\ 1_2^+$ B(GT) for 5.7 MeV is small and was not measured

$(g_A^{eff}/g_V)^2 = 1.272^{-0.010}_{+0.010(stat)+0.013(syst)}$ theoretical estimation of $B(GT)\ 1_2^+/B(GT)_{tot} \leq 0.01$

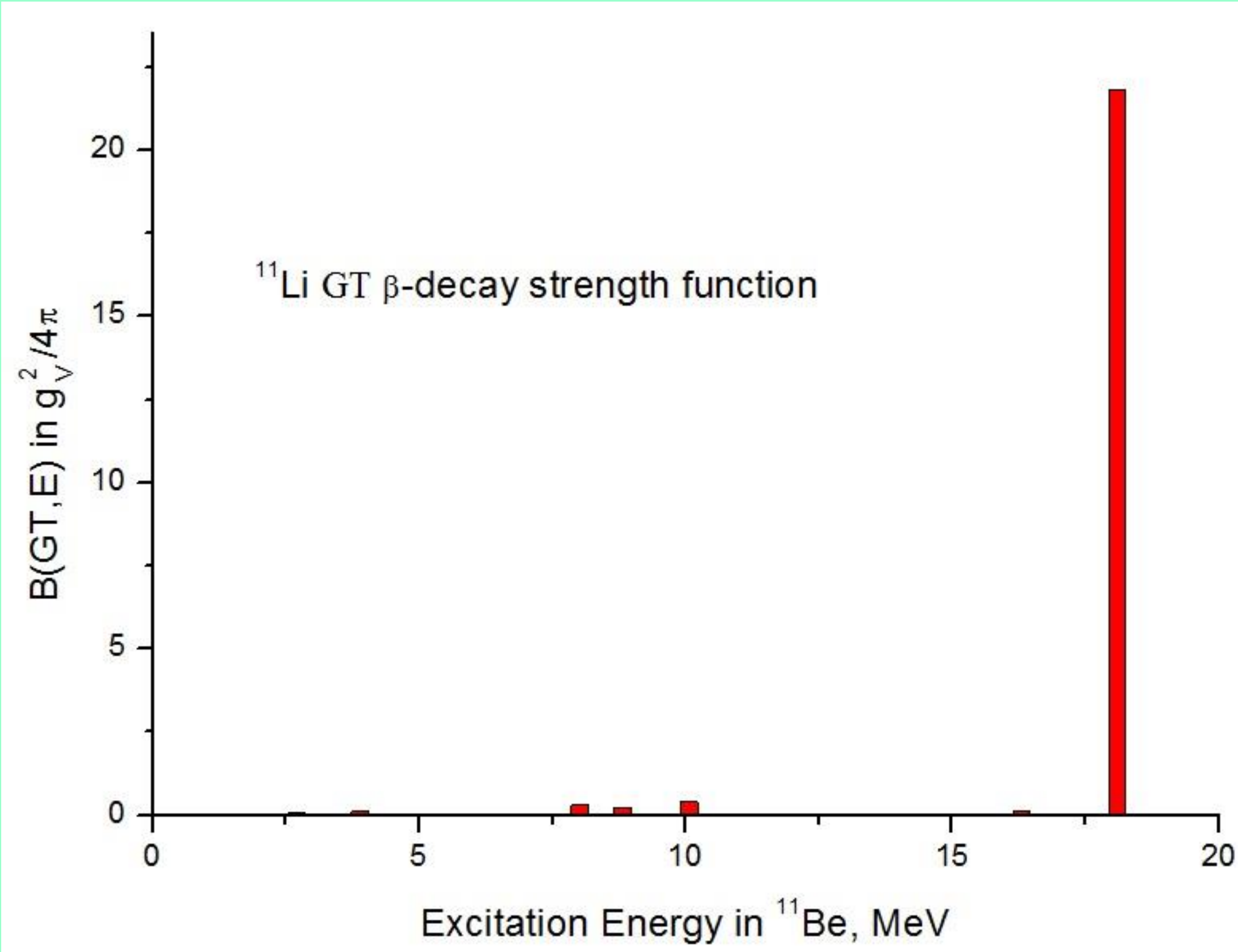

^{11}Li GT β-decay strength function
B(GT,E) in $g_V^2/4\pi$
Excitation Energy in ^{11}Be, MeV
0
5
10
15
20

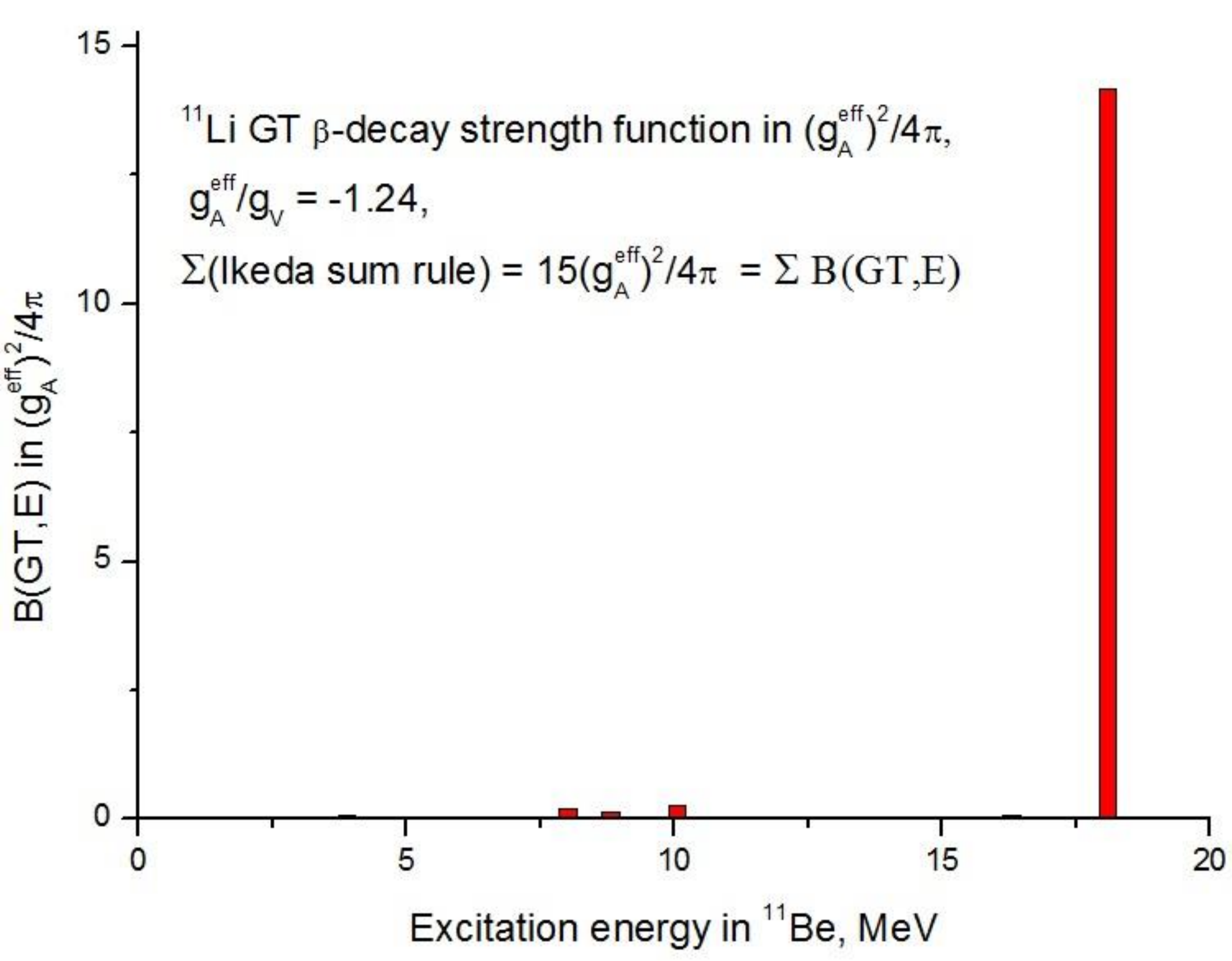

^{11}Li GT β-decay strength function in $(g_A^{eff})^2/4\pi$,
g_A^{eff}/g_V = -1.24,
Σ(Ikeda sum rule) = $15(g_A^{eff})^2/4\pi$ = Σ B(GT,E)
B(GT,E) in $(g_A^{eff})^2/4\pi$
Excitation energy in ^{11}Be, MeV
0
5
10
15
20

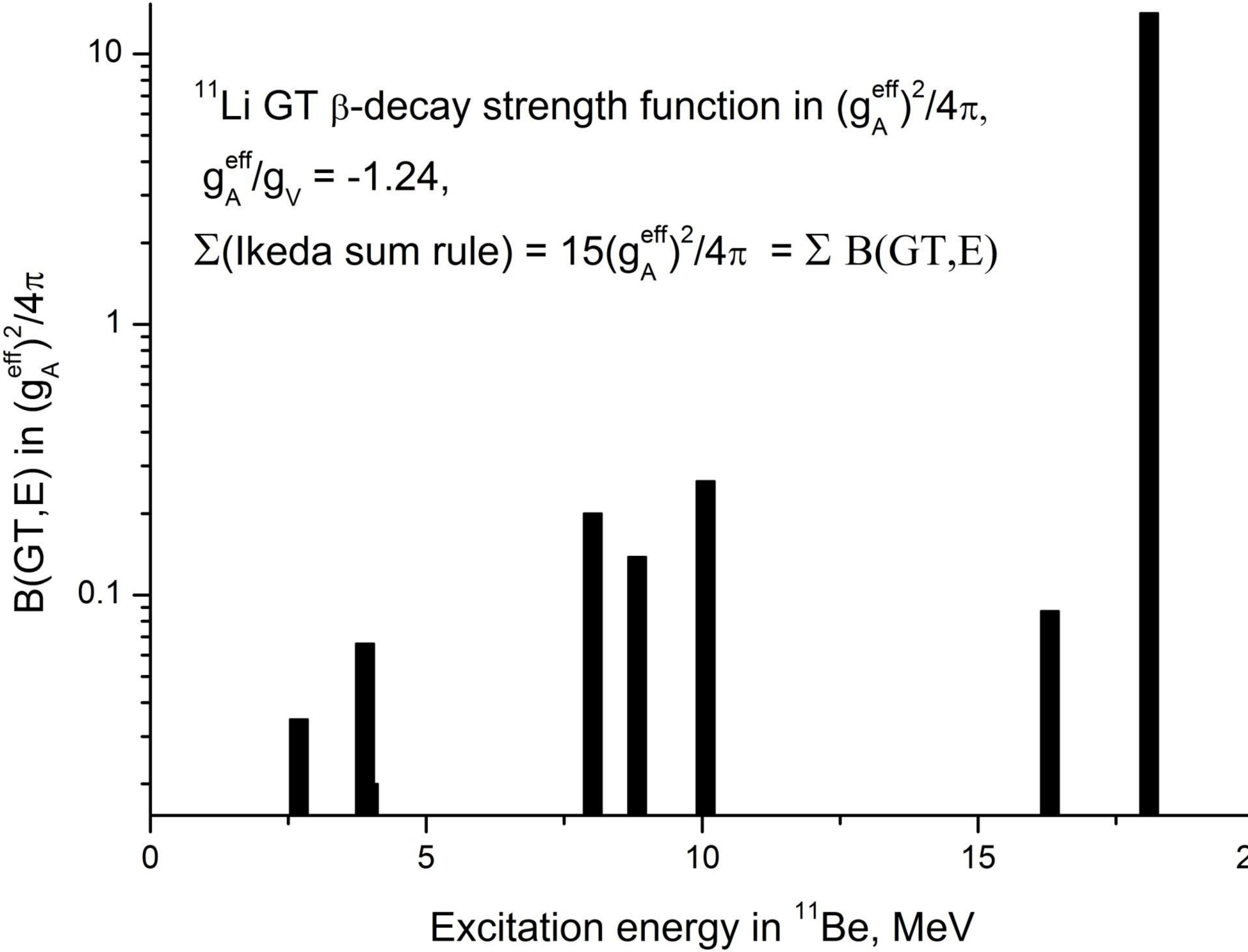

^{11}Li GT β-decay strength function in $(g_A^{eff})^2/4\pi$,
$g_A^{eff}/g_V = -1.24$,
Σ(Ikeda sum rule) = $15(g_A^{eff})^2/4\pi = \Sigma\, B(GT,E)$
B(GT,E) in $(g_A^{eff})^2/4\pi$
10
1
0.1
0
5
10
15
20
Excitation energy in ^{11}Be, MeV

^{11}Li g.s. (T = T_Z = 5/2; J^π =3/2$^-$) β – decay scheme, g_A^{eff}/g_V = -1.24. Level energies in ^{11}Be, E_{GT}=18.19 MeV, lg*ft* =2.45(13) , E_{IAR} = 21.16 MeV (J^π=3/2$^-$;T = 5/2, T_Z = 3/2).

β – decay to ^{11}Be, $E_{lev,}$ MeV	J^π	Branching ratio (%)	lg *ft*	*B*(GT) in $g_V^2/4\pi$	*B*(GT) in $g^{eff}{}_A{}^2/4\pi$
0.32	1/2$^-$	7.7±0.8	5.67±0.04	0.013	0.008
2.69	3/2$^-$	17±4	5.06±0.10	0.053	0.034
3.41	(3/2$^-$)	0.9±0.4	6.25±0.10	0.003	0.002
3.890±0.001	5/2–	22.7±4.5	4.78±010	0.102	0.066
$3.969^{+0.02}_{-0.0009}$	3/2$^-$	6.8±2.4	5.30±0.20	0.030	0.020
5.24	5/2$^-$	2.4±0.5	5.55±0.08	0.017	0.011
7.03	(5/2$^-$)	0.86±0.17	5.77±0.09	0.010	0.006
8.02±0.02	3/2$^-$	15.5±3.1	4.30±0.08	0.308	0.200
8.82	3/2$^-$	8.9±1.4	4.46±0.07	0.213	0.138
10.06	5/2$^-$	7.8±1.8	4.18±0.12	0.406	0.263
16.3		0.048±0.007	4.66±0.08	0.134	0.087
18.1		0.55±0.06	2.45±0.13	21.810	14.162
				Σ=23.1 in $g_V^2/4\pi$	**Ikeda Σ=15$g_A^2/4\pi$**

Compare experimental total strength for β-decay in $g_V^2/4\pi$ units with the Ikeda sum rule (in $(g_A^{eff})^2/4\pi$ units), we obtained **$(g_A^{eff}/g_V)^2$ = 1.272 ± 0.010 for ^{6}He** GT β$^-$-decay and **$(g_A^{eff}/g_V)^2$ = 1.5±0.2 for ^{11}Li** GT β$^-$-decay.

One of the consequence of the Wigner spin-isospin SU(4) symmetry is

$$E_{\mathrm{GT}} = E_{\mathrm{IAR}}.$$

SU(4) symmetry-restoration effect induced by the residual interaction,

which **displaces the GT towards the IAR with increasing (N-Z)/A**.

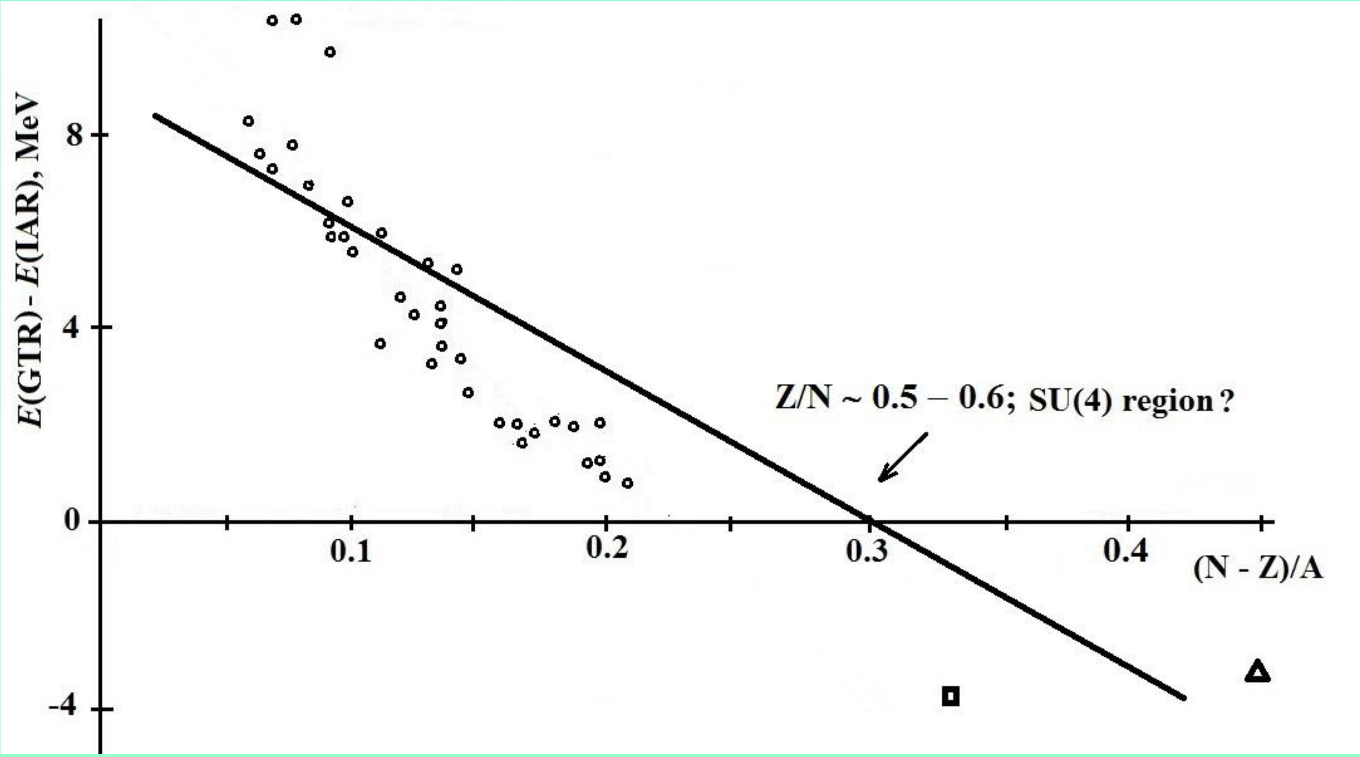

The difference of the E_{GT} - E_{IAR} energies (circles) as a function of the neutron excess [*Naumov Yu.V., Bykov A.A., Izosimov I.N.* Structure of β-decay strength functions // Sov. J. Part. Nucl. 1983. V.14, No 2. P.175.;
Izosimov I.N. Non-Statistical Effects Manifestation in Atomic Nuclei // Physics of Particles and Nuclei. 1999. V. 30, No 2. P.131.].

Data for ^{6}He β^{-} – decay was (square) and ^{11}Li β^{-} – decay (triangle) were added.

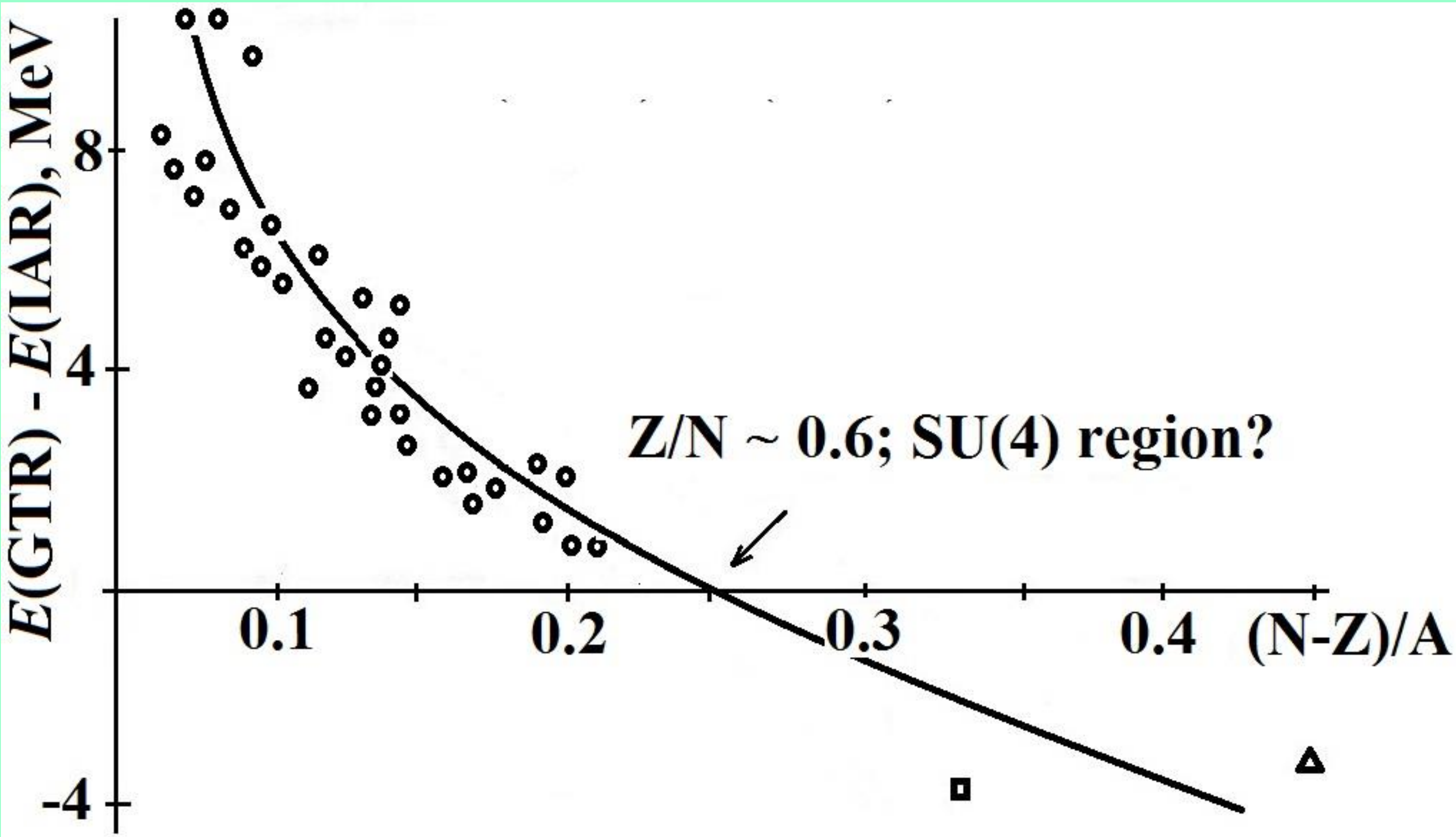
E(GTR) - E(IAR), MeV
8
4
-4
0.1
0.2
0.3
0.4
(N-Z)/A
Z/N ~ 0.6; SU(4) region?

CONCLUSION

1. **Gamow-Teller resonance and pygmy resonances** in GT beta decay strength function $S_\beta(E)$ for halo nuclei may have structure corresponding to ***np* tango** halo. When neutron excess is high enough, resonances in $S_\beta(E)$ may **simultaneously have both *nn* Borromean halo component and *np* tango halo** component and form so-called mixed halo.

2. Ratio of axial-vector and vector weak interaction constants for the beta decay of halo nuclei (^{6}He, ^{11}Li) from Σ 1/*f*t may be obtained. $\mathbf{(g_A^{eff}/g_V)^2 = 1.272 \pm 0.010}$ **for ^{6}He** GT β^--decay and $\mathbf{(g_A^{eff}/g_V)^2 = 1.5 \pm 0.2}$ **for ^{11}Li** GT β^--decay.

3. Structure of resonances in $S_\beta(E)$ is manifested in charge exchange reactions. Halo structure of some pygmy resonances is important for beta-decay analysis in halo nuclei.

4. Value **Z/N ≈ 0.5 - 0.6** may correspond to the **SU(4) spin-isospin symmetry region**.

In the ground state, the ^{6}**Li** nucleus has an ***α* + *d* cluster structure**, the energy of its breakup to an alpha particle and a **deuteron being as low as 1.47 MeV**. The radius of the ^{6}Li nucleus ranges between **2.32 and 2.45 fm**; this is approximately **10% larger** than the value expected according to standard ($\sim A^{1/3}$) systematics. The momentum distributions of residual nuclei arising as breakup products were studied in for various targets and various energies of ^{6}He and ^{6}Li beams. This resulted in observing, for ^{4}He nuclei, a rather narrow (**σ = 28–29 MeV s^{-1}**) distribution in the case of ^{6}He breakup and a distribution of intermediate width (**σ = 46–55 MeV s^{-1}**) in the case of ^{6}Li breakup. For ordinary nuclei (that is those without a halo), the width of the momentum distribution of breakup products is **$\sigma \sim$ 100 MeV s^{-1}**. Rather narrow momentum distributions of breakup products confirm the presence of a halo in the ^{6}He nucleus and the hypothesis that the **^{6}Li nucleus has a tango halo.**

The even–even nucleus ${}^6_2\mathrm{He}_4$ offers an enlightening example of configuration mixing. The nucleus can be described as a two-particle nucleus with two neutrons in the 0p shell. All states of this model space have $T = 1$.

$$\{|1\rangle\,,\,|2\rangle\} = \{|(\nu 0\mathrm{p}_{3/2})^2\,;\,0^+\rangle\,,\,|(\nu 0\mathrm{p}_{1/2})^2\,;\,0^+\rangle\}$$

^{6}He halo neutrons: $(p_{3/2})^2$ with a 7% admixture of $(p_{1/2})^2$ configuration

<u>^{11}Li nucleus (nn halo)</u>

Two neutrons that form the nn halo occupy the 1s and 0p orbits. The ^{11}Li ground state wave function has the form

$$\| \Psi({}^{11}Li) > \approx \| \Psi({}^{9}Li) \otimes 2n > , \qquad (3)$$

$$\| \Psi({}^{9}Li) \otimes 2n > \approx a_s \| \Psi({}^{9}Li) \otimes (1s_{1/2})^2 > + a_p \| \Psi({}^{9}Li) \otimes (0p_{1/2})^2 > .$$

^{11}Li halo neutrons (55(10)% $(0p_{1/2})^2$, 45(10)% $(1s_{1/2})^2$

S. Yoshida, et al. Phys. Rev. C97,054321 (2018)

One of the interesting features of the present shell-model results is that the GTGR energy can be lower than the IAS energy, i.e. E(GT) – E(IAS) < 0 for very neutron-rich nuclei.

It is thus very interesting to measure the evolution of E(GT) – E(IAS) toward very neutron-rich nuclei using radioactive isotope beams.

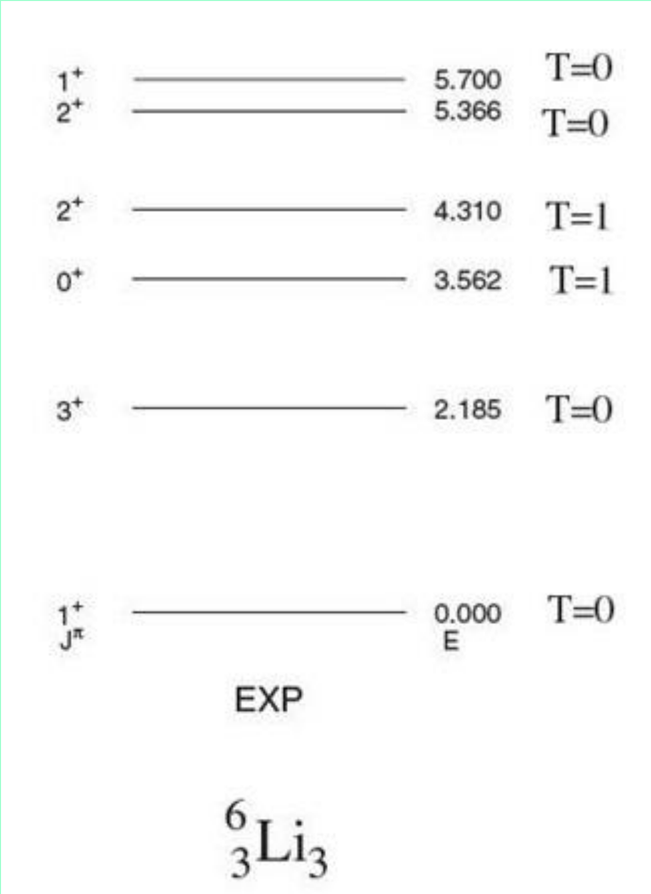

Y. Fujita, Y. Utsuno, H. Fujita
Properties of Low-energy Super Gamow-Teller State, JPS Conf. Proc. **23**, 012030 (2018)

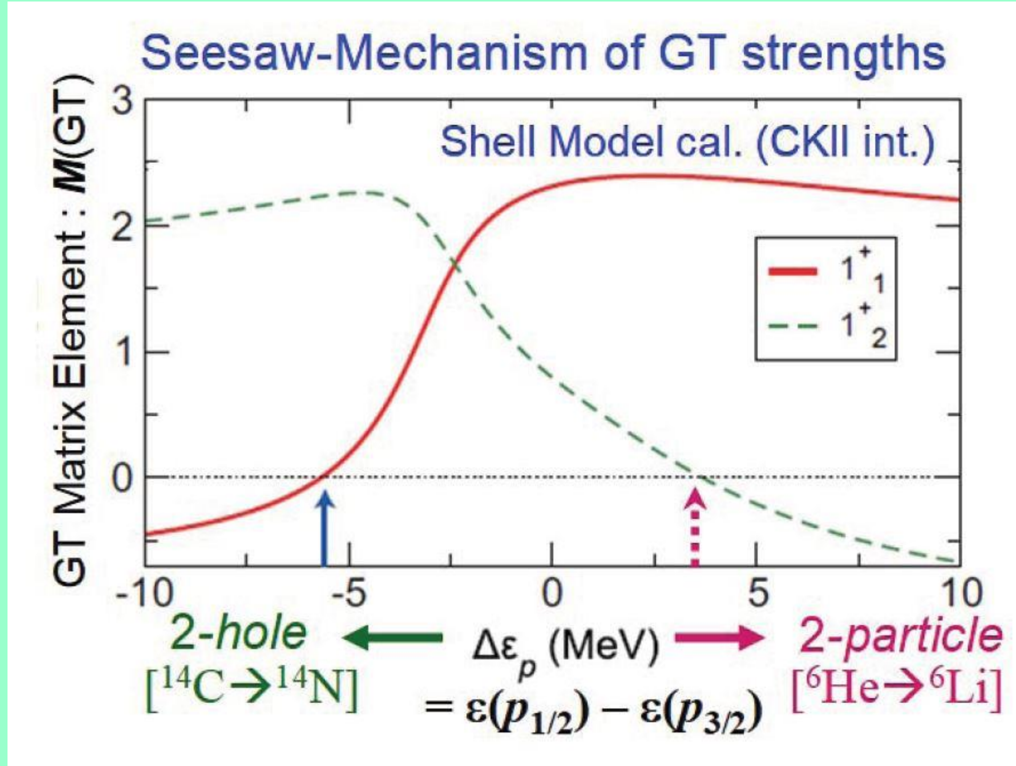

$\Delta\varepsilon_{ls} \approx 1.4\ V_{ls}\ (\mathbf{l{\cdot}s})\ A^{-2/3}$, $\Delta\varepsilon_{ls}(p_{1/2}-p_{3/2}) \approx 6$ MeV for ^{6}Li

$\rightarrow$ M(GT)1_2^+/M(GT)$_{tot}$ ≤ 0.1 $\rightarrow$ B(GT) 1_2^+/B(GT)$_{tot}$ ≤ 0.01 for ^{6}Li, E(1_2^+) = 5.7 MeV,

$(g_A^{eff}/g_V)^2 = 1.272 \pm 0.010$, without B(GT) 1_2^+

$(g_A^{eff}/g_V)^2 = 1.272^{-0.010}_{+0.010(stat)+0.013(syst)}$ theoretical estimation of B(GT) 1_2^+/B(GT)$_{tot}$ ≤ 0.01

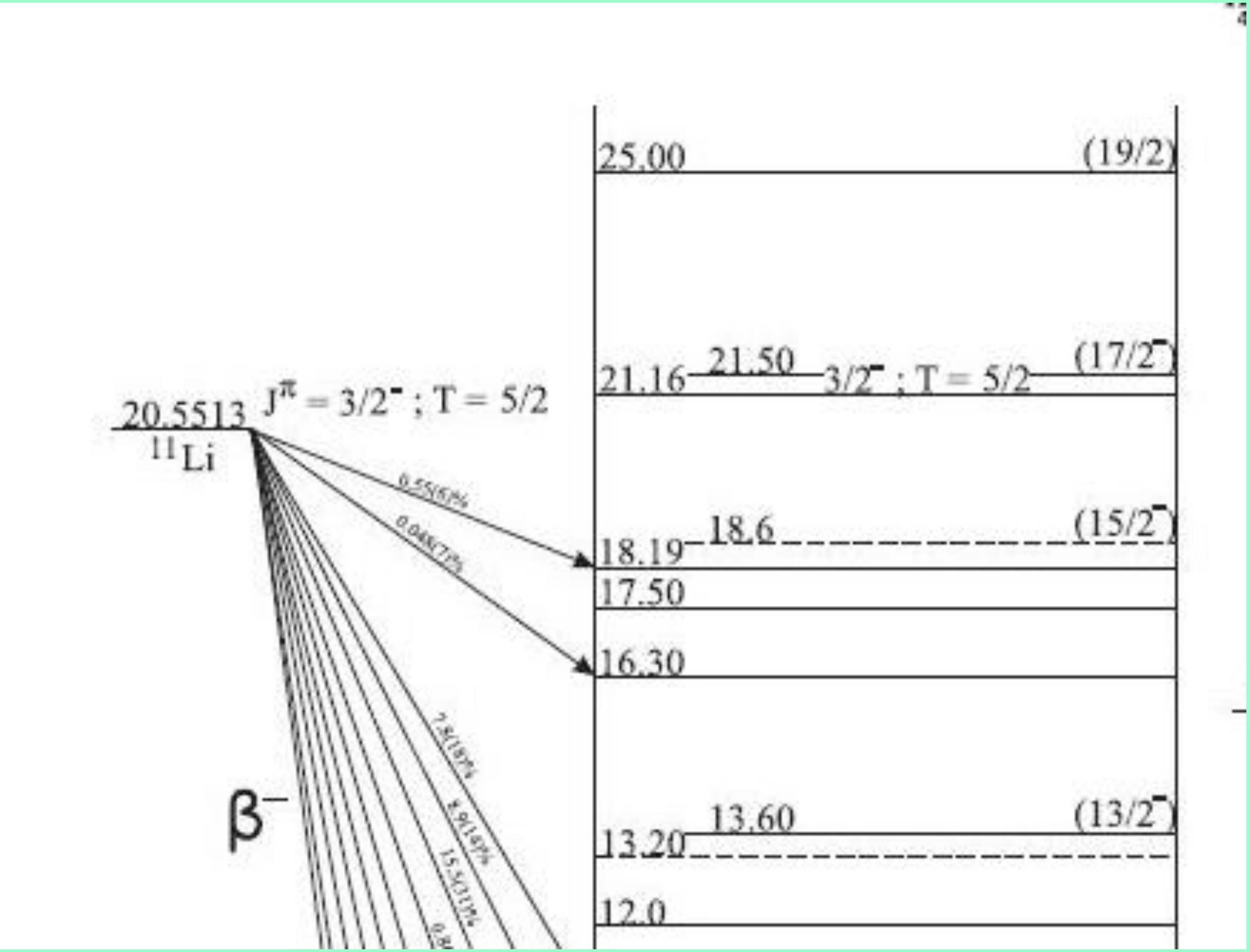

No observed additional GT states (or GT resonance components)

The conserved vector-current hypothesis (CVC) and partially conserved axial-vector-current hypothesis (PCAC) yield the free-nucleon [10] value g_A/g_V = -1.27. Inside nuclear matter the effective value $g^{eff}{}_A$ is needed to reproduce experimental observations. Precise information on the value of $g_A{}^{eff}$ is crucial when predicting half-life for beta- decays, beta - decay strength function for Gamow-Teller (GT) and first forbidden (FF) beta-transitions, and cross section for charge exchange reactions. The effective value of $g_A{}^{eff}$ is characterized by a renormalization factor q (in the case of quenching of g_A it is called quenching factor): $q=g_A{}^{eff}/g_A{}^{free}$, where $g_A{}^{free}$ = -1.2723(23) is the free-nucleon value of the axial-vector coupling measured in neutron beta decay and $g_A{}^{eff}$ is the value of the axial-vector coupling derived from a given theoretical or experimental analysis.

The renormalization of g_A which stems from the nuclear-model effects depends on the nuclear-theory framework chosen to describe the nuclear many-body wave functions involved in the weak processes. This is why the effective values of g_A^{eff} can vary from one nuclear model to the other. The origin of the quenching of the g_A value is not completely known and various mechanisms have been proposed for its origin including tensor effects, the Δ-isobar admixture to the nuclear wave function, relativistic corrections to the Gamow-Teller operator, etc., but a clean separation of these aspects is difficult.

Also, the experimental methods of quenching value determination in many cases may have essential uncertainties. One of the model independent methods for g_A^{eff} determination is the comparison of the experimental total GT beta decay strength with the Ikeda sum rule. **For application of this method it is necessary to have the total GT strength in the energy window allowed for beta decay.** Such situation may be realized for beta decay of halo nuclei (^{6}He, ^{11}Li) or for very neutron-rich nuclei where $E_{\mathrm{GTR}} < E_{\mathrm{IAR}}$.

The possible halos for beta-stable nuclei may occur as excited states with energies close to the neutron separation energy. Otherwise the halo binding energy would be too large. Moving towards the dripline, halos may occur as low-lying excitations or as the nuclear ground state.

The first excited states of ^{11}Be and ^{17}F are referred to as the halo states.

Strong coupling to other more complicated states dilute the component of the halo and might effectively prevent its occurrence. In other words, the distance between nonhalolike many-body states must be larger than the coupling to the halo state (or level density is not high).
High level density of nonhalolike levels prevent halo formation.

Excited halo states may also occur with excitation energy below nucleon separation energy by at most 1 MeV.

If these states are not surrounded by many other excited states, they could represent halos provided the quantum numbers and the structure in general are correct.

The isobaric analog states of a halo could be candidates for excited halo states, since they have the same structure as the original state except for the exchange of neutrons and protons.

Isospin symmetry prevents mixing of states with different isospin quantum number. Isobar Analog States may have halo structure at high excitation energy.

The three most studied halo nuclei are ^{6}He, ^{11}Li and ^{11}Be. However, a few others have also now been confirmed, such as ^{14}Be, ^{14}B, ^{15}C and ^{19}C.
All the above are examples of neutron halo systems, and all lie on, or are close to, the neutron dripline at the limits of particle stability.

Other candidates, awaiting proper theoretical study and experimental confirmation include ^{15}B, ^{17}B and ^{19}B, along with ^{22}C and ^{23}O.

Proton halo nuclei are not quite as impressive in terms of the extent of their halo, due to the confining Coulomb barrier which holds them closer to the core. Nevertheless, examples include ^{8}B, ^{12}N, ^{17}Ne and the first excited state of ^{17}F.

In the general case the IAS is the coherent superposition of the excitations like neutron hole–proton particle coupled to form the momentum $J = 0^+$. The IAS has the isospin $T=T_z+1=(N-Z)/2+1$, where $T_z = (N - Z)/2$ is the isospin projection. The isospin of the ground state is $T = T_z = (N - Z)/2$. When the IAS energy corresponds to the continuum, the IAS can be observed as a resonance.

Configuration states (CS) are not the coherent superposition of such excitations and have $T = T_z = (N - Z)/2$. One of the best studied CS is the anti-analog state (AIAS). The CS formation may be restricted by the Pauli principle.

The Double Isobar Analog State (DIAS) has the isospin $T = T_z + 2$ and is formed as the coherent superposition of the excitations like two neutron holes–two proton particles coupled to form the momentum $J = 0^+$.

When the nuclear parent state has the two-neutron (*nn*) Borromean halo structure, then IAR and configuration states (CSs) can simultaneously have *nn*, *np* Borromean halo components in their wave functions. After *M*1 γ-decay of IAR with *np* Borromean halo structure or GT β^--decay of parent nuclei with *nn* Borromean halo structure, the states with *np* halo structure of tango type may be populated.

The strength function $S_\beta(E)$ governs the nuclear energy distribution of elementary charge-exchange excitations and their combinations like proton particle (πp)-neutron hole (νh) coupled into a spin-parity Iπ : [πp ⊗ νh]Iπ and neutron particle (νp)-proton hole (πh) coupled into a spin-parity Iπ : [νp ⊗ πh)]Iπ. The strength function of Fermi-type β-transitions takes into account excitations [πp ⊗ νh]0+ or [νp ⊗ πh]0+. Since isospin is a quite good quantum number, the strength of the Fermi-type transitions is concentrated in the region of the isobar-analogue resonance (IAR). The strength function for β-transitions of the Gamow–Teller (GT) type describes excitations [πp ⊗ νh]1+ or [νp ⊗ πh]1+. Residual interaction can cause collectivization of these configurations and occurrence of resonances in $S_\beta(E)$.

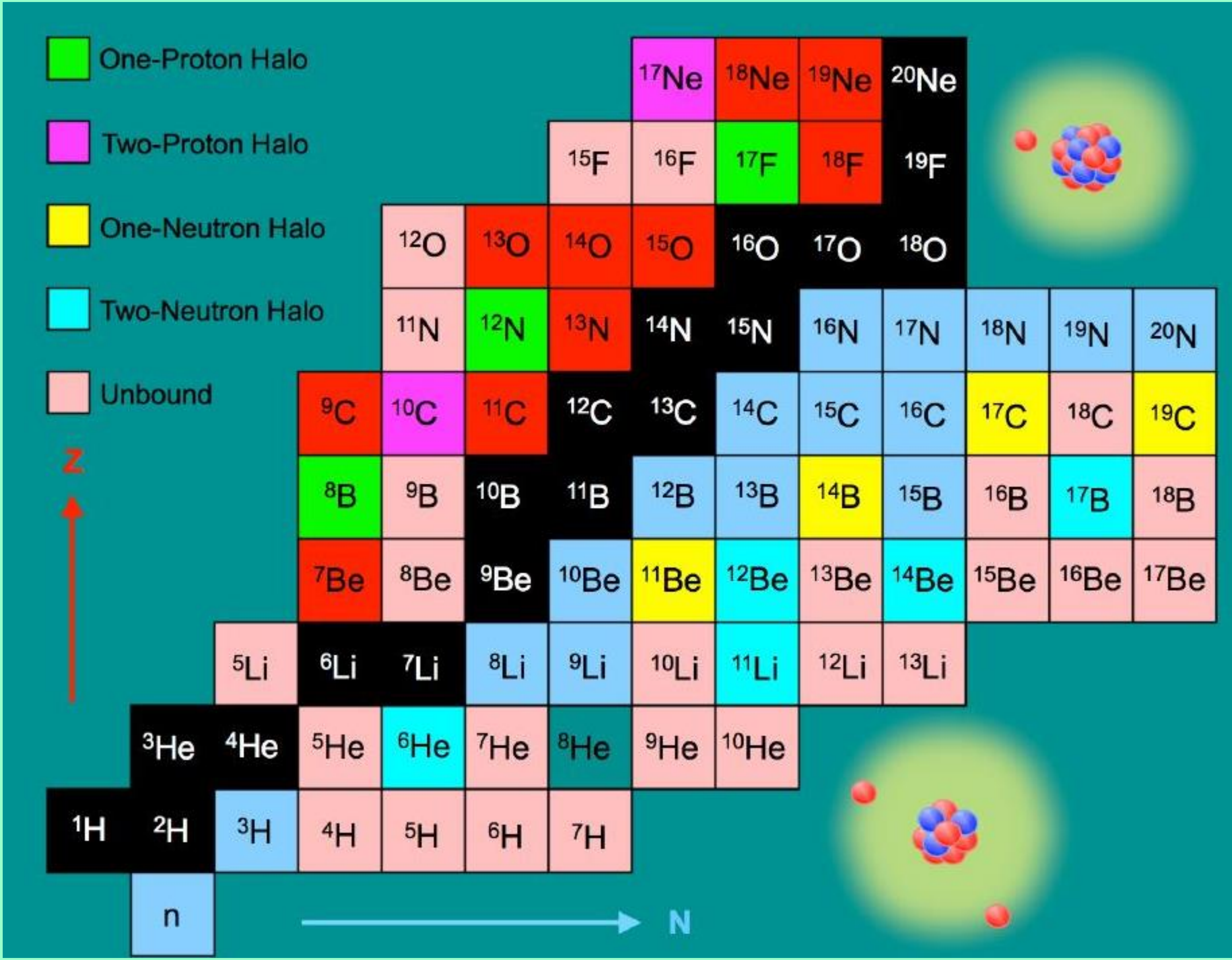

One-Proton Halo
Two-Proton Halo
One-Neutron Halo
Two-Neutron Halo
Unbound
Z
N
^{17}Ne ^{18}Ne ^{19}Ne ^{20}Ne
^{15}F ^{16}F ^{17}F ^{18}F ^{19}F
^{12}O ^{13}O ^{14}O ^{15}O ^{16}O ^{17}O ^{18}O
^{11}N ^{12}N ^{13}N ^{14}N ^{15}N ^{16}N ^{17}N ^{18}N ^{19}N ^{20}N
^{9}C ^{10}C ^{11}C ^{12}C ^{13}C ^{14}C ^{15}C ^{16}C ^{17}C ^{18}C ^{19}C
^{8}B ^{9}B ^{10}B ^{11}B ^{12}B ^{13}B ^{14}B ^{15}B ^{16}B ^{17}B ^{18}B
^{7}Be ^{8}Be ^{9}Be ^{10}Be ^{11}Be ^{12}Be ^{13}Be ^{14}Be ^{15}Be ^{16}Be ^{17}Be
^{5}Li ^{6}Li ^{7}Li ^{8}Li ^{9}Li ^{10}Li ^{11}Li ^{12}Li ^{13}Li
^{3}He ^{4}He ^{5}He ^{6}He ^{7}He ^{8}He ^{9}He ^{10}He
^{1}H ^{2}H ^{3}H ^{4}H ^{5}H ^{6}H ^{7}H
n

There may be only a small window open for halo occurrence.

How small can be answered by understanding the transition from ordinary nuclei via clusters to halos and study halo in excited states.

The existence of close- or lowlying thresholds is not a sufficient condition for formation of a halo.

Although halo structures could also be present in excited states (halo isomers), but they are easier to observe and have therefore mainly been investigated in ground states.

As halo states should be close to a threshold this implies one is close to the nucleon drip lines;

Since proton halos are retarded by the Coulomb barrier the neutron drip line will offer more cases.

In atomic nucleus whose ground state does not exhibit halo structure, but the excited state may have one, the γ-transition from the excited state to the ground state can be essentially hindered, i.e. the formation of a **specific type of isomers (halo isomers) becomes possible**.

Also halo isomer formation becomes possible when the halo structure of the excited states is different.

neutron leaks into
classically forbidden region

- Large radii and dilute surface
- Low-momentum components
- Bound-state and continuum sector not well separated (very few bound states)
- Decoupling of valence nucleons and core
- Reduced Spin-Orbit splitting (~ 1/r dV/dr)

low **angular momentum motion for halo particles and few-body dynamics**

In halo nuclei, magic numbers lose their magicity!

And new magic numbers appear.

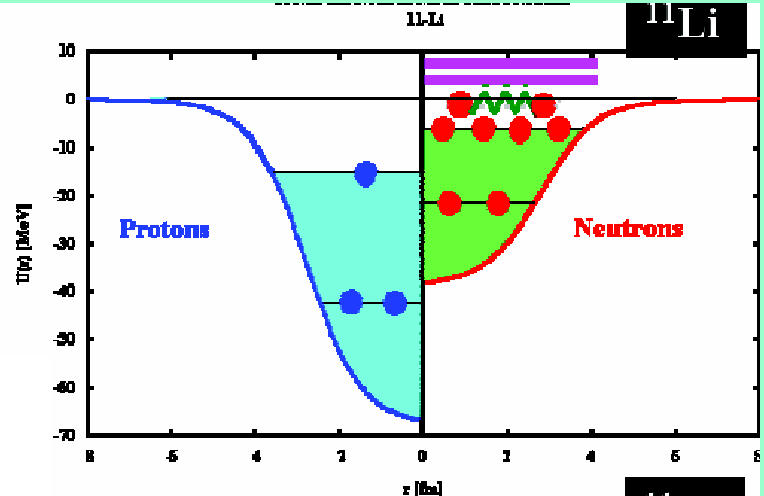

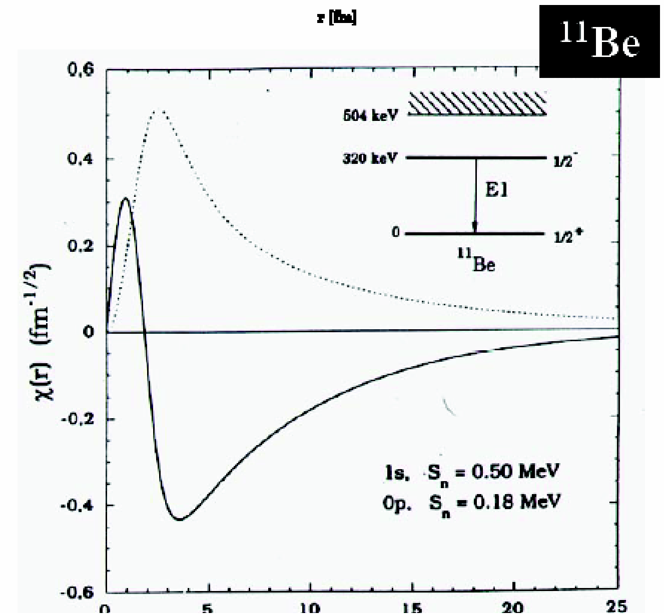

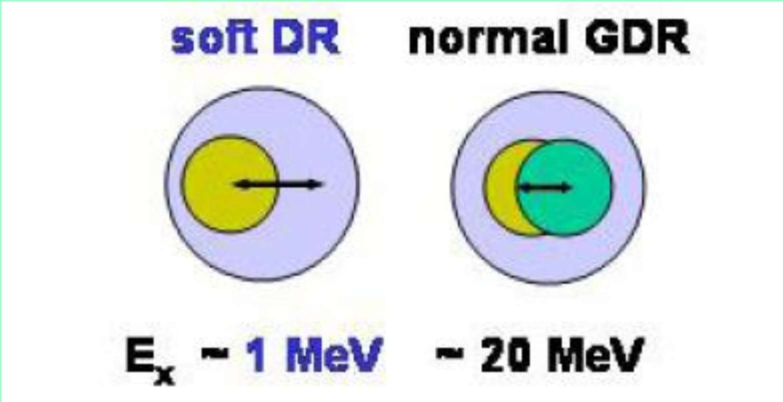

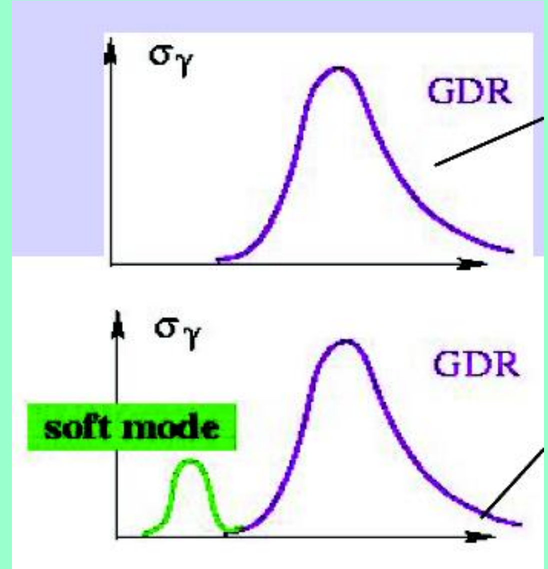

excitations of soft modes with

- different multipolarity
- collective excitations *versus* direct transition from weakly bound to continuum states

$$\sigma_\gamma(E_X) = \frac{16\pi^3}{9\hbar c} E_X \frac{dB(E1)}{dE_X}$$

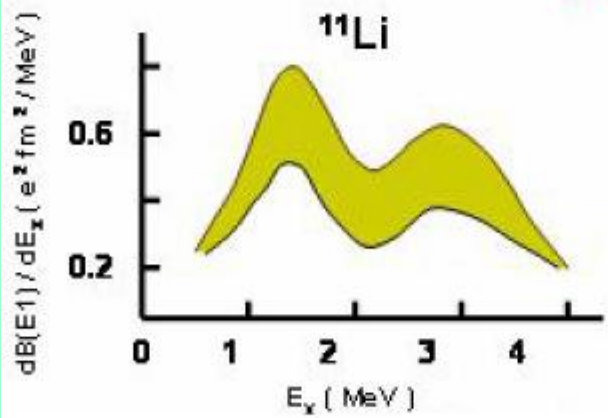

M. Zinser et al., Nucl. Phys. A619 (1997) 151

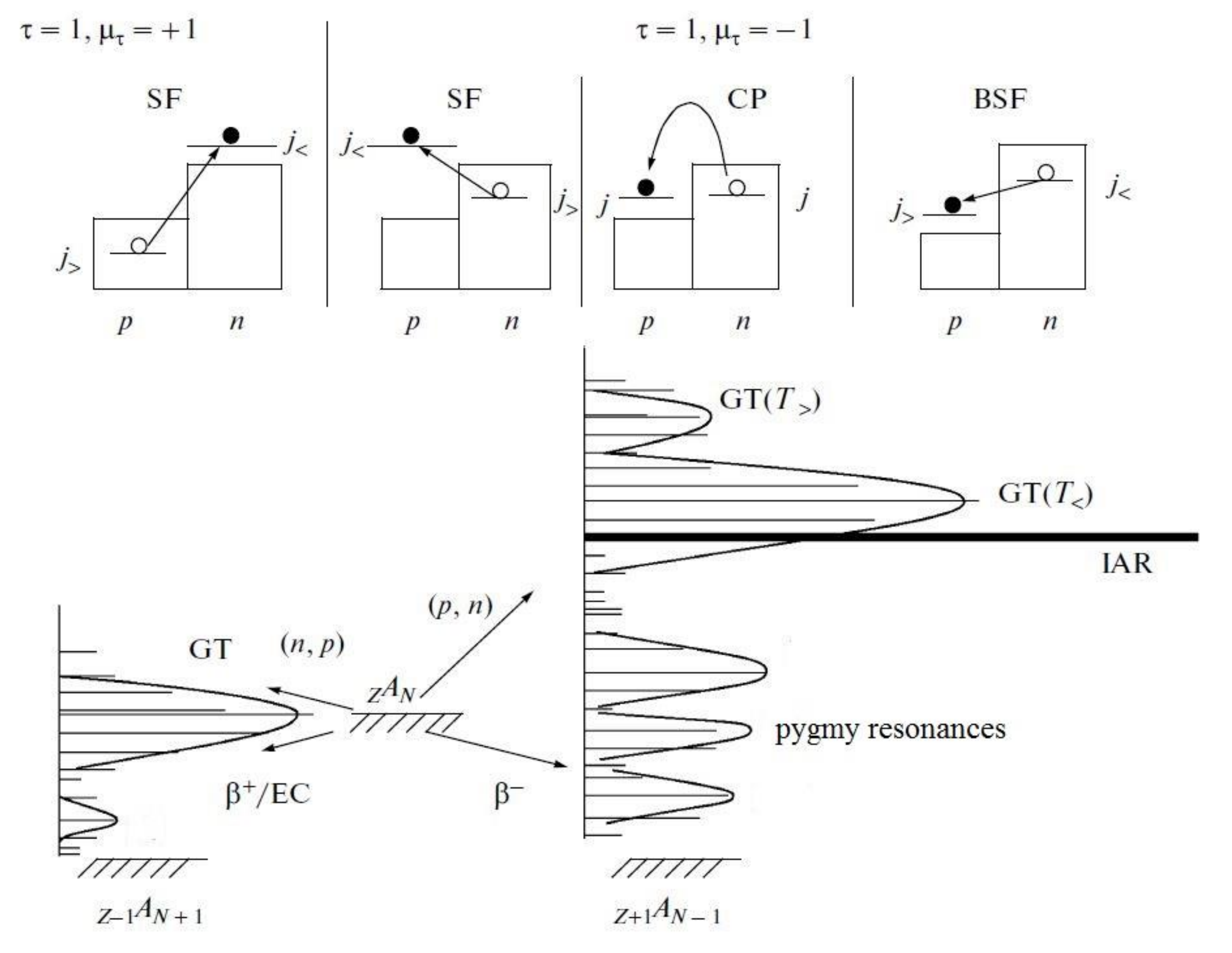

Diagram of strength functions for GT β transitions and configurations that form resonances in $S_\beta(E)$ for GT transitions, where $j_> = l + 1/2$, $j_< = l - 1/2$, τ – isospin of excitation, μ_τ – projection of isospin. The strength of the Fermi-type transitions is concentrated in the region of the isobar-analogue resonance.

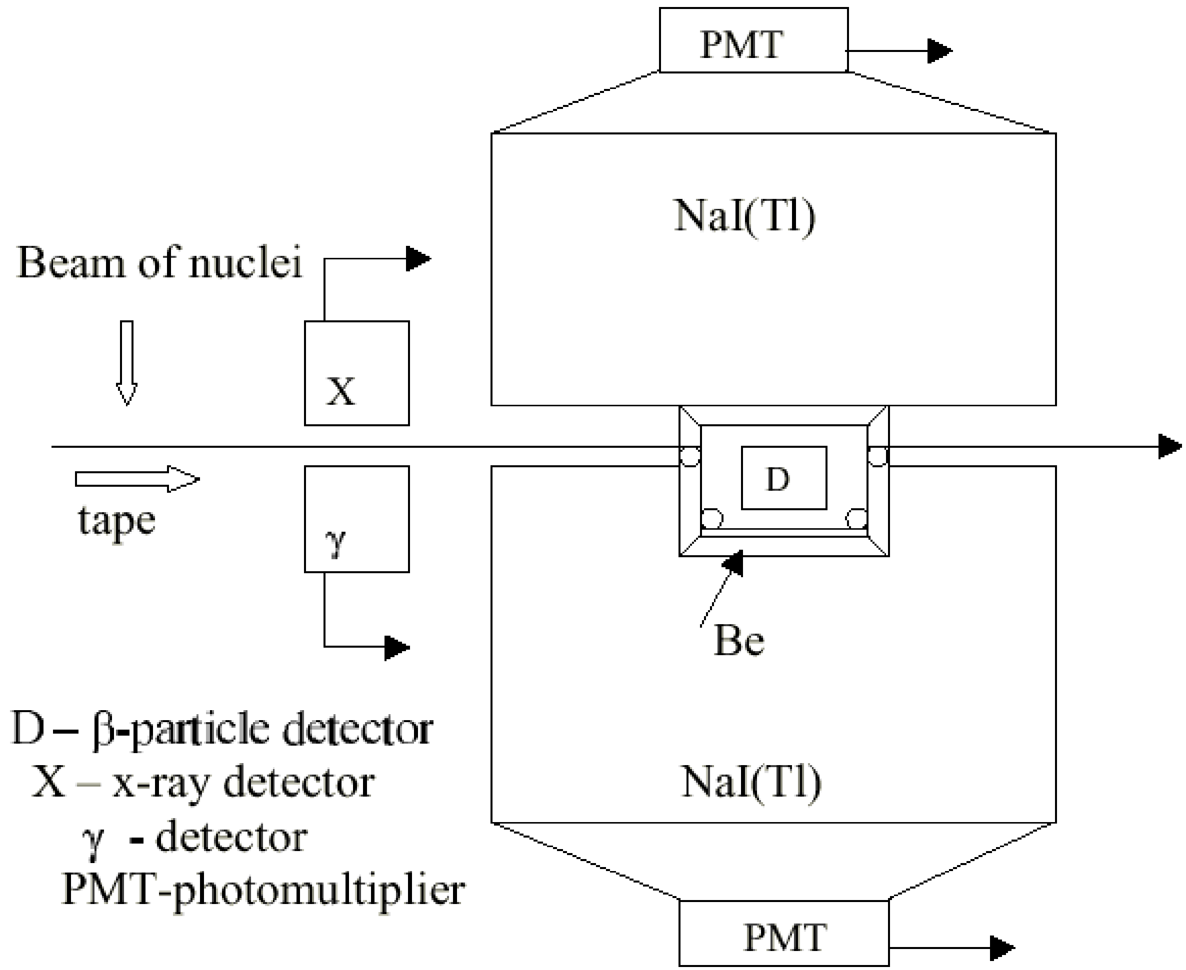
PMT
NaI(Tl)
Beam of nuclei
X
D
tape
γ
Be
D – β-particle detector
X – x-ray detector
γ - detector
PMT-photomultiplier
NaI(Tl)
PMT

$S_\beta(E)$ study by TAS spectroscopy:

1. Direct measurement of the levels populations after β-decay **I(E)** ⟹ $\mathbf{S_\beta(E)}$
3. 4π geometry
4. Photoefficiency $\varepsilon_{ph} = \exp(-\alpha E)$

⟹ for total-absorption peaks the total absorption efficiency $\boldsymbol{\varepsilon_{ta}}$: $\boldsymbol{\varepsilon_{ta}(E)} = \boldsymbol{\varepsilon_{ph}(E)}$, and not depend on decay scheme details.

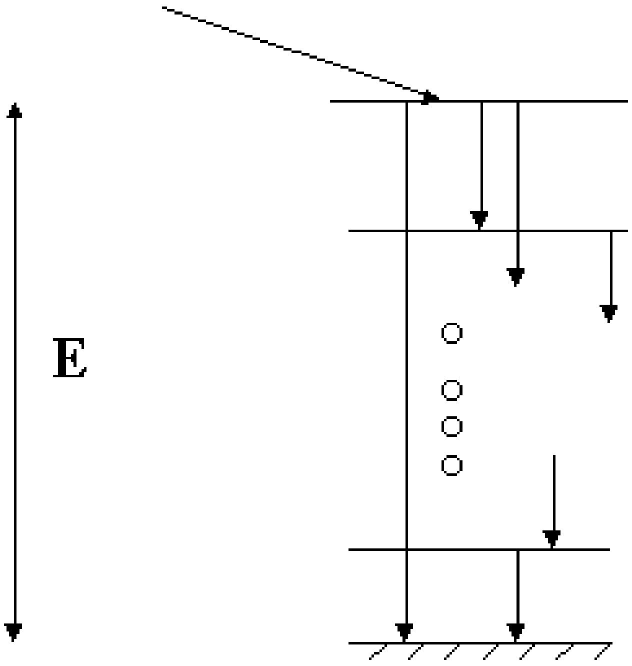

Indeed, if we have a deexcitation scheme for a level with energy E populated by the β decay, then, if relation (**4.**) holds true, the detection efficiency for the total absorption peak for a cascade of n γ rays with the total energy $E = E_{\gamma 1} + ... + E_{\gamma n}$ is defined as

$$\begin{aligned} \varepsilon_{\mathrm{tot}}(E) &= \exp(-\alpha E_{\gamma 1}) \times \ldots \times \exp(-\alpha E_{\gamma n}) \\ &= \exp(-\alpha(E_{\gamma 1} + \ldots + E_{\gamma n})) = \exp(-\alpha E), \end{aligned} \tag{7}$$

and does not depend on the scheme of γ transitions

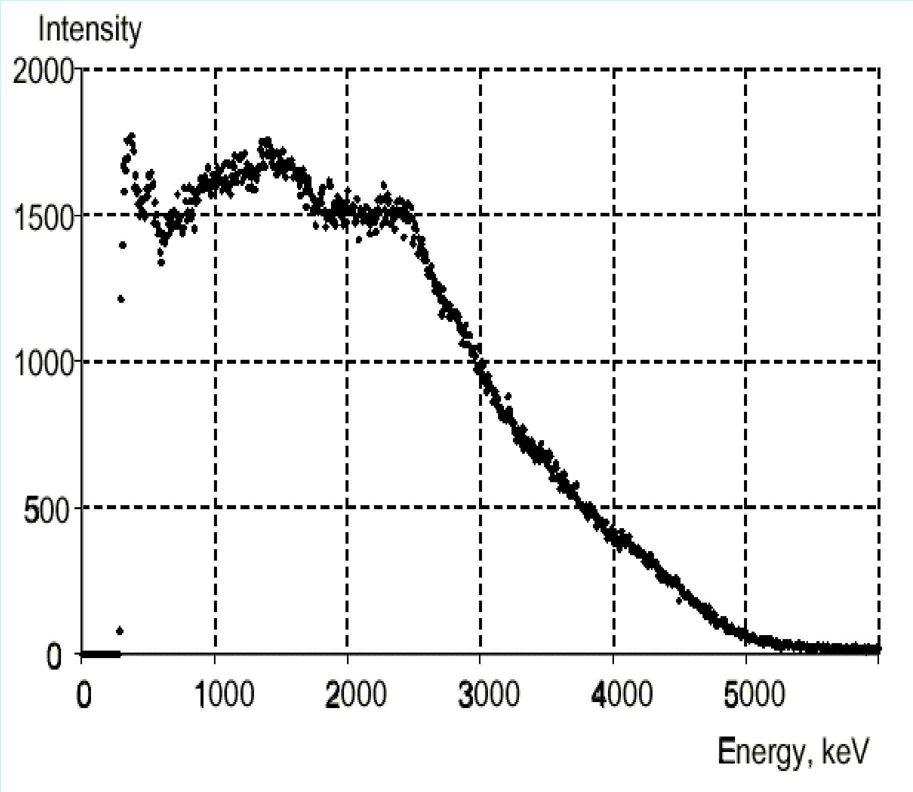

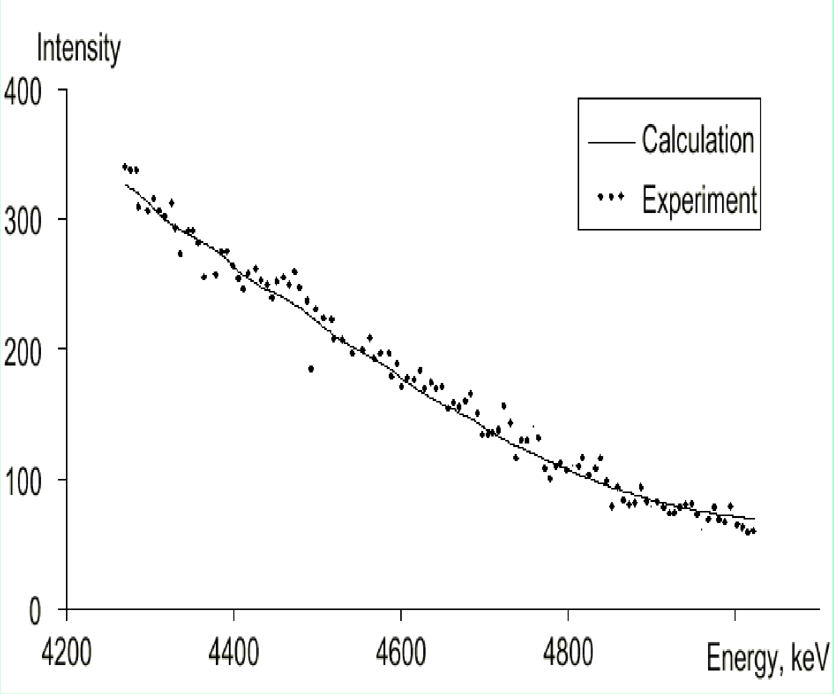

Experimental (*a*) and fitted (*b*) TAS spectra of 156-Ho (*T*1/2 *≈56min)*

Q_{EC}=(5.05±0.07)MeV

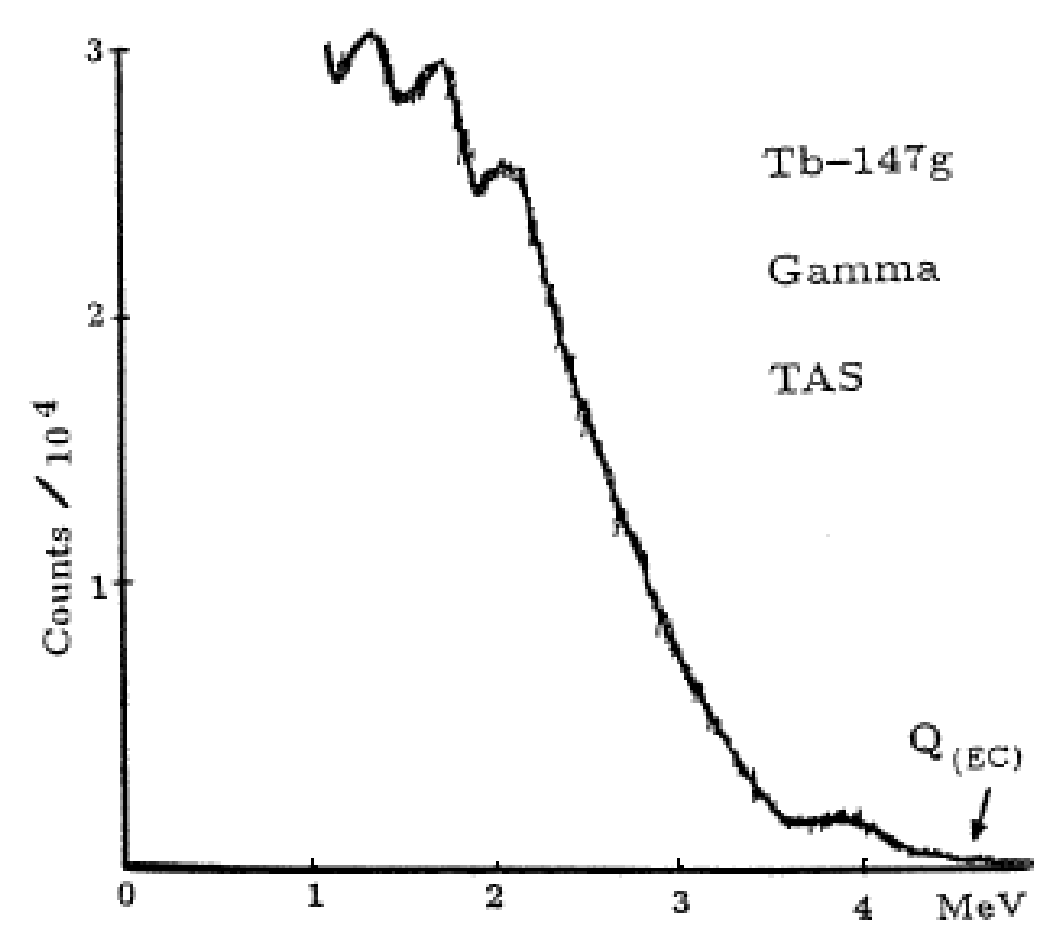
Tb–147g
Gamma
TAS
Counts / 10^4
3
2
1
0
1
2
3
4
MeV
Q (EC)

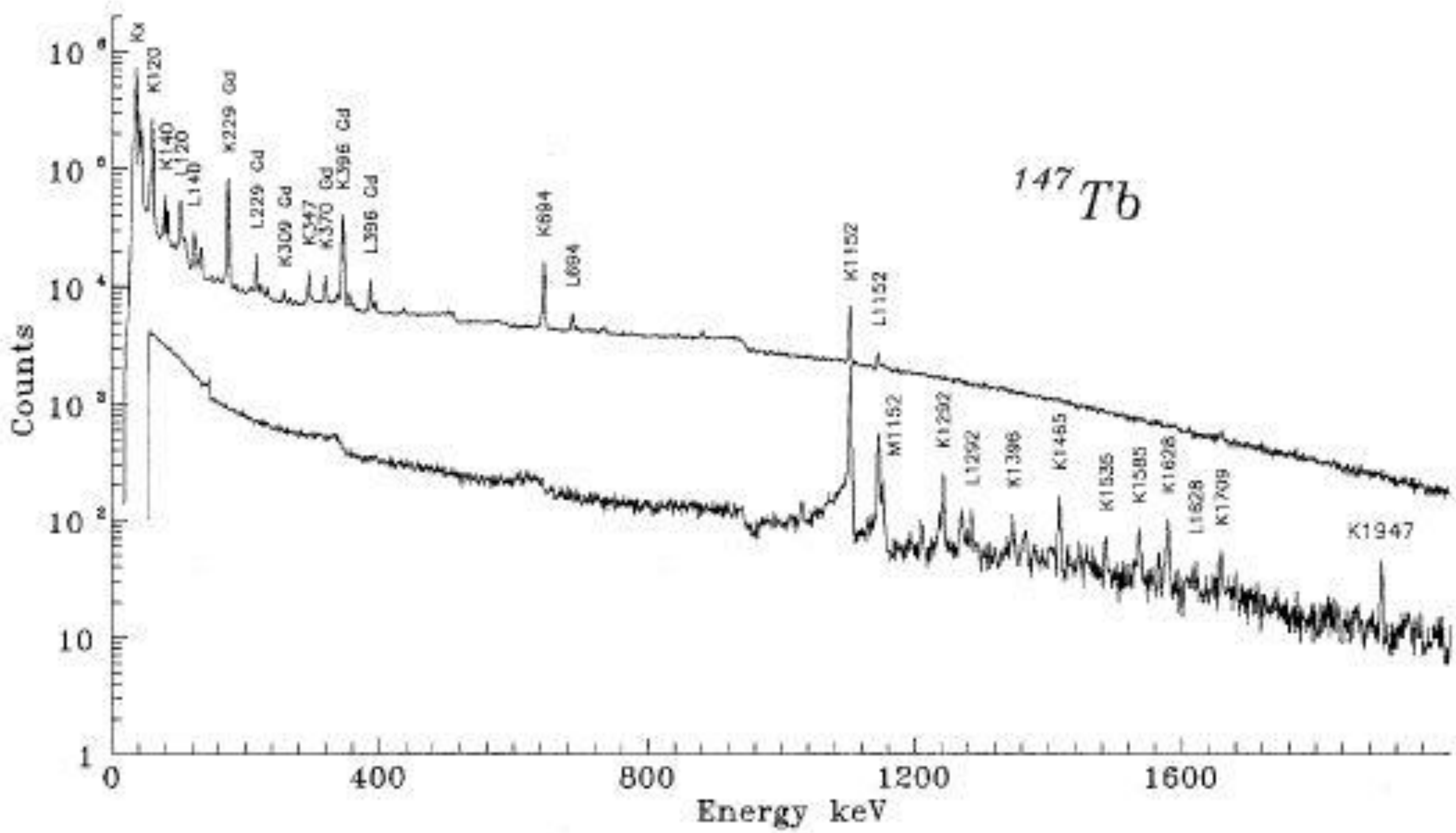

Fig. 2. Spectra of the internal conversion electrons at the decay of ^{147g}Tb, measured with a miniorange magnetic filter (*bottom*) and without it (*top*)

Table 1. Recommended upper limit for B(E,λ) or B(M,λ) in W.u.

$\Gamma\gamma/\Gamma_w$=B(E,λ) /B(E,λ)$_w$ or B(M,λ)/B(M,λ)$_w$, $\Gamma\gamma$ - gamma width.

$\Gamma\gamma/\Gamma_w$ upper limit

transition*	A=6 - 44$	A=45 - 150	A>150
E1 (IV)	0,3#	0,01	0,01
E2 (IS)e	100	300	1000
E3	100	100	100
E4	100	100@	
M1 (IV)	10	3	2
M2 (IV)	3	1	1
M3 (IV)	10	10	10
M4		30	10

'w' – Weisskopf estimates, W.u. – Weisskopf unit.

* 'IV' and 'IS' - isovector or isoscalar.

@ $\Gamma\gamma/\Gamma_w$(upper limit)=30 for A=90-150.

\# $\Gamma\gamma/\Gamma_w$(upper limit)=0,1 for A=21-44.

$ $\Gamma\gamma/\Gamma_w$(upper limit)=10-for E2 (IV); 0,03 - for M1 (IS); 0,1 - for M2 (IS); 0,003 for E1 (T=0 states ,due to isospin mixture).

e For super deformed bands $\Gamma\gamma/\Gamma_w$>1000 for E2 gamma transitions may be observed.